Federal University of Goiás

Institute of Physics

Quantum Optics and Information Group

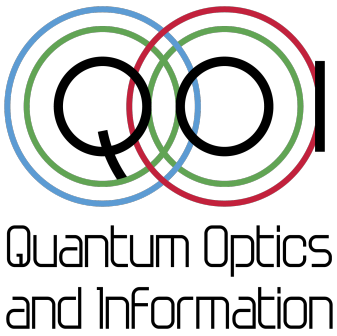

A Brief Study of Quantum Computation via Nuclear Magnetic Resonance

Undergraduate Thesis

Letícia Lira Tacca

Goiânia-GO, December, 2019

Brazil

Dedication

I dedicate this work to my kitten Rey, this being of light who accompanies me every day and gives me the purest love of which only animals are capable of, without asking anything in return. Well, maybe a meat sac from time to time ...

... and to all the people who helped me through all these years.

Acknowledgments

Many are the people I would like to thank, many beyond what I remember right away. Without them I would not have expanded my mind in so many ways.

I thank my family for their unconditional support and understanding. My mother Noelma, for the sacrifices she made, always thinking first of her daughters, before herself. My grandmother Norberta, who raised me as her own daughter and taught me all the virtues I have. To my father Selvino, who even distant helps me with what I need and teaches me to live simply. To my late grandfather Moises, who even in dreams shows me that the bonds of love are eternal. My aunt Nelminha, uncle Calil, Gabriel, Jeanny, Arthurzinho and Joyce, for always welcoming me with open doors and being my family at all times.

To my best friends ever, Yuna, Paulo, Pedro, Raphaela, Thais and Gean, who for years endure my follies and sufferings and are always there when I need it or not. You are my soul brothers and sisters.

And all my cousins, uncles and aunts.

Many thanks to my colleagues who helped me on this long and arduous journey. Among them, Silvia, Kauara, Jennyfer, Leticia, Juliane, Luiz Henrique, Janine, Rafael, Walbert, Arthur, Julio, Caio, Gabriela, Gabriel, and many other names from all IF courses. Without them, I would understand almost nothing about physics.

Also thanks to my colleagues at the 4^{th} EAFexp, Amanda, Ana Flávia, Jéferson, Leonardo, Marcos, Nina, and Professors Roberto Sarthour and Alexandre Souza for all help, time, attention, independence and patience during the program. Also to dear monitor Filipe Melo for all assistance and commitment to help us.

To my teachers, among them a special thanks to the teachers Jose Nicodemos and Andreia Luisa, for guiding me in several years of the Scientific Initiation program. You paved my way for physics research. And in particular, I thank Professor Lucas Chibebe very much for accepting to be my life counselor and advisor.

I thank my girlfriend Ana Carollina very much, for always being by my side and understanding when I can not be. Thank you for all the support, affection and love in recent months.

And last but not least, I thank not only the people who were part of this path by my side, but also the books I read, because everything I learned from them is a good part of who I am and want to be.

ABSTRACT

This monograph briefly discusses some basic ideas on Quantum Computation and how some of its applications are realized. In particular, the technique of Nuclear Magnetic Resonance is used to study spin states through Hamiltonian simulations. In addition, a study of Bell's entangled states is performed, without pretense of originality, in order to demonstrate how to implement a quantum circuit using a real quantum computer, namely the ©IBM Q Experience quantum processor.

Contents

List of Figures

Chapter 1

Introduction

In an article written in 1981 [1], Richard Feynman discussed the issue of simulating physics with computers. What are the possibilities offered by computation? What kind of computer would be used to successfully simulate the laws of Nature? Or a deeper question, can we simulate physics with a *universal computer*? What kind of physics would we imitate? Although our everyday experience limits us to an approximately classical world, which we can satisfactorily describe with local differential equations, in essence the physical world is quantum mechanical. Seen in this way, our most primordial goal is the question of how to simulate quantum mechanics and what kind of computation is needed for it.

"Classical" computing, as its name implies, is appropriate when we want to study the physical world limited by classical approximations. But what does this mean? This means that a classical, or conventional computer (just like the one on which I write this monograph), is subject to restrictions that prevent it from using all the possibilities that physical theory provides us for solving computational problems. Quantum computing, on the other hand, utilizes the full potential of quantum mechanics to its advantage, making it one of the most powerful tools in the task of simulating nature with due accuracy. In fact, a quantum computer does exactly the same calculations as a conventional computer. However, the simulation of quantum mechanical processes in physics, chemistry and biology is performed exponentially faster in a quantum computer, making it much more efficient in many applications.

The characterization of quantum states of a system is one of the most important tools of Quantum Mechanics and in particular of Quantum Computation (QC). The latter, unlike its

classic counterpart, can use quantum systems of two levels that present in addition to binary states (0 and 1), superposition states, and based on this, perform the implementation of logic gates, algorithms and quantum information. At a more fundamental level, a theory of information based on quantum principles extends and completes classical information theory, just as complex numbers extend and complete real numbers.

The race for *quantum supremacy* [2,3] is in vogue today, and a lot of money is being invested year after year in technology companies and advanced research centers so that the full mastery of this powerful computing tool will be a reality for days to come. In 2017 IBM announced the construction of a quantum chip containing 50 qubits, and in March 2018 Google announced another quantum chip containing 72 qubits [4]. This year, the latter announced that it had achieved supremacy. There are many companies around the world involved in this technology race, which makes this research area one of the most promising in the coming years.

Several platforms are already used to perform quantum computation, among them are quantum processors based on atomic traps, superconducting circuits, and the Nuclear Magnetic Resonance technique. The latter is the object of study of this work, which is based on the work I did, along with colleagues from various corners of the country at the 4^{th} EAFexp - CBPF, in February 2019; it aimed to study quantum information processing via Nuclear Magnetic Resonance (NMR) through nuclear spin states.

In order for the concepts behind quantum computation via NMR to be well spelled out, this monograph was divided into four main chapters. Chapter 2 provides a brief explanation of the fundamental concepts of quantum mechanics and their postulates for both pure state vector and density operator optics. Chapter 3 focuses on describing the fundamentals of quantum computing, starting from the theory of entanglement in composite systems, going through a brief description of quantum bits and a discussion of quantum coherence, and finally, describing some logical operations and how quantum gates are used to implement simple quantum circuits. In Chapter 4 we present the principles of resonance theory and how the NMR technique works; a description of the experimental setup used is given. Finally, in Chapter 5, an application of quantum computing are demonstrated, by showing how NMR can be used for Hamiltonian simulation. In the appendices, an implementation on IBM's quantum computer is performed to study entangled Bell states.

Chapter 2

Quantum mechanics

A physical theory [5] provides a well-grounded description of a physical phenomenon. Such a description is possible only after several hypotheses are confirmed by tests and experiments performed with high levels of confidence. Moreover, a physical theory is itself a "maternal box" of tools, which, when developed, allow us a broader understanding of the phenomenon in question. By equipping ourselves with such tools, we can apply the most appropriate mathematical formalism and structure the foundations that support the postulates that are the laws of physics.

Quantum Mechanics (QM) is a physical theory that emerged in the early twentieth century as a result of the need to explain certain physical phenomena that could not be explained with current classical theories, such as *blackbody radiation* and *stable electron orbits* [6]. It is named after predicting the phenomenon of electron energy quantization, which classical theory cannot describe. However, quantum theory is not limited to describing only microscopic phenomena, it is also extremely important in explaining macroscopic phenomena, since the microscopic behavior of matter is quantized. QM is the basis of various fields of physics and chemistry, and its foundations were laid during the first half of the twentieth century by a number of renowned physicists such as Max Planck, Albert Einstein, Niels Bohr, Werner Heisenberg, Louis de Broglie, Erwin Schrodinger, Paul Dirac, Max Born, Richard Feynman, among others.

2.1 The postulates of quantum mechanics

In physics, we consider as a *system* a fragment of reality that has been separated for study. It is a very useful abstraction that helps us to understand in a general way a certain physical

phenomenon. A *quantum system* can generally be understood as a class of procedures prepared in such a way that can be verified by proper testing [7]. This system supports descriptions that use quantum theory, such as molecules and atoms.

When studying a physical system, we specify its properties and, from them, it is possible to know how a given system behaves over time. Because physical systems are not static, they evolve so that the same system, prepared in the same way, can give rise to distinct experimental results. This dynamic property leads us to analyze such a system through a concept of *state*. But what really is this "state"? We can define a state as a mathematical quantity that determines all values of the physical properties of a system associated with it at any given time. In other words, *all information that can be known in a given system constitutes its state.* However, this is a somewhat vague definition. If we consider a given preparation and suitable configuration of tests to be performed on a quantum system many times, then we have that a probabilistic distribution for the outputs of these tests converges to a limit. Therefore, we can define a quantum state as follows: *A state is characterized by the probabilities of the various outcomes of every conceivable test.* [7]

2.1.1 State space

The postulates of QM define the state of the system according to its vector space, how this state evolves in time, and how we can measure it, given that we will have a set of many states, which forms a probability distribution. The first one sets up the arena in which quantum mechanics takes place. The arena is the projective Hilbert space [8].

Postulate 1. *Associated to any isolated physical system is a complex vector space, with an inner product defined on it, known as the state space of the system. The system is completely described by its state vector, which is normalized to unity.*

In the space of functions, the state would be described by the wave function, $\Psi(x,t)$, instead of the state vector $|\psi\rangle$. The latter is composed of sequences of complex numbers or functions. The internal product that characterizes the Hilbert space provides us with information about angles and distances. By performing linear transformations between state vectors through *operators*, we obtain their rotations and translations. Operators also describe physical quantities such as *position*, *linear momentum*, *angular momentum* and *energy*.

Phase

For any complex number written in polar form, the phase factor is a complex exponential ($e^{i\theta}$) that multiplies a ket $|\psi\rangle$ or a bra $\langle\phi|$. For example, let us consider the state $e^{i\theta}|\psi\rangle$, where $|\psi\rangle$ is a state vector and θ is a real number. We say that the state $e^{i\theta}|\psi\rangle$ is equal to $|\psi\rangle$, up to the *global phase factor* $e^{i\theta}$. Therefore, both vectors represent the same physical system.

2.1.2 Evolution

The second postulate describes how the state of a quantum mechanical system evolves with time.

Postulate 2. *The time evolution of the state of a closed quantum system is determined by the Schrödinger equation,*

$$i\hbar\frac{d|\psi\rangle}{dt} = H|\psi\rangle\,. \tag{2.1}$$

In this equation, $\hbar = h/2\pi$ and h is a physical constant known as Planck's constant, whose value must be experimentally determined. H is a fixed Hermitian operator known as the Hamiltonian of the closed system.

The Hamiltonian (energy) operator is Hermitian, and so are the other operators associated with physical quantities. In order to show this, we need to recall that the Hamiltonian is composed of two parts, a kinetic energy and a set of potential energy terms. The first one carries a momentum operator p, and the second one involves the coordinates x, y etc. We can prove that the various terms comprising the Hamiltonian are Hermitian then the whole Hamiltonian is Hermitian.

The state $|\psi\rangle$ of the system at time t_1 is related to the state $|\psi'\rangle$ of the system at time t_2 by a unitary operator U which depends only on the times t_1 and t_2,

$$|\psi'\rangle = U(t_2, t_1)|\psi\rangle\,, \tag{2.2}$$

where $U(t_2, t_1)$ is the *time evolution operator*, given by:

$$U = e^{-i\mathcal{H}t/\hbar}. \tag{2.3}$$

Postulate 2 demands that the system being described be closed. Although the universe is a closed system as a whole, in fact all the systems that we can interact in the world are open. That is, they interact with other systems. Nevertheless, there are interesting systems which can be described to a good approximation as being closed, which are described by unitary evolution.

Because the Hamiltonian is an Hermitian operator, it has a spectral decomposition in the form

$$H = \sum_E E \left|E\right\rangle \left\langle E\right| , \tag{2.4}$$

with eigenvalues E and corresponding normalized eigenvectors $|E\rangle$. The states $|E\rangle$ are conventionally referred to as *energy eigenstates*, or sometimes as *stationary states*, and E is the energy of the state $|E\rangle$. The lowest energy is known as the *ground state energy* for the system, and the corresponding energy eigenstate (or eigenspace) is known as the *ground state*. The reason the states $|E\rangle$ are sometimes known as stationary states is because their only changes in time is to acquire an overall numerical factor

$$\left|E\right\rangle \rightarrow \exp\{-iEt/\hbar\} \left|E\right\rangle . \tag{2.5}$$

2.1.3 Quantum measurement

Despite we postulate that our quantum system must be closed and evolving according to unitary evolution, when an observation is made to find out what is going on inside the system, there is an interaction with experimental equipment, an interaction that makes the system no longer closed, and thus not necessarily subject to a unitary evolution. The third postulate describes the effects of measurements on quantum systems.

Postulate 3. *Quantum measurements are described by a collection M_m of measurement operators. These are operators acting on the state space of the system being measured. The index m refers to the measurement outcomes that may occur in the experiment. If the state of the quantum system is $|\psi\rangle$ immediately before the measurement then the probability that the outcome m occurs is given by*

$$p(m) = \left\langle \psi\right| M_m^\dagger M_m \left|\psi\right\rangle , \tag{2.6}$$

and the state of the system after the measurement is

$$|\psi'\rangle = \frac{M_m |\psi\rangle}{\sqrt{\langle\psi| M_m^\dagger M_m |\psi\rangle}}. \tag{2.7}$$

The measurement operators satisfy the completeness relation,

$$\sum_m M_m^\dagger M_m = I, \tag{2.8}$$

that ensure probability conservation

$$1 = \sum_m p(m) = \sum_m \langle\psi| M_m^\dagger M_m |\psi\rangle . \tag{2.9}$$

Projective measurements

Projective measurements are a special case of Postulate 3. It can be described by an *observable*, M, a Hermitian operator on the state space of the system being observed [8]. The observable has a spectral decomposition

$$M = \sum_m m P_m, \tag{2.10}$$

where P_m is the projector onto the eigenspace of M with eigenvalue m. The possible outcomes of the measurement correspond to the eigenvalues, m, of the observable. The probability of getting the result m after the measurement of the state $|\psi\rangle$ is given by

$$p(m) = \langle\psi| P_m |\psi\rangle , \tag{2.11}$$

and the state of the quantum system immediately after the measurement is

$$|\psi'\rangle = \frac{P_m |\psi\rangle}{\sqrt{P_m}}. \tag{2.12}$$

We can also define the average value of the measure as

$$\langle M\rangle \equiv \langle\psi| M |\psi\rangle . \tag{2.13}$$

From this formula for the average follows a formula for the standard deviation associated to observations of M

$$[\Delta(M)]^2 = \langle (M - \langle M \rangle)^2 \rangle = \langle M^2 \rangle - \langle M \rangle^2 \tag{2.14}$$

General Measurements (POVM)

For several applications, we are not interested in the post-measurement state of the system, but on the probabilities of the respective measurement outcomes. It happens, for example, in experiments where the system is measured only once. In such instances there is a mathematical tool known as the *POVM ('Positive Operator-Valued Measure') formalism* which is especially well adapted to the analysis of the measurements.

Suppose we define

$$E_m \equiv M_m^\dagger M_m, \tag{2.15}$$

where M_m are measurement operators that describe a measurement performed upon a quantum system in the state $|\psi\rangle$. The outcome m has a probability given by $p(m) = \langle\psi| M_m^\dagger M_m |\psi\rangle$. From Postulate 3 and linear algebra, E_m is a positive operator such that

$$\sum_m E_m = I, \tag{2.16}$$

$$p(m) = \langle\psi| E_m |\psi\rangle . \tag{2.17}$$

Therefore the set of operators E_m are sufficient to determine the probabilities of the different measurement outcomes. The operators E_m are known as the *POVM elements* associated with the measurement. The complete set E_m is known as a *POVM* [8].

2.1.4 Distinguishing quantum states

Classicaly, we are able to distinguish different states of information, at least in principle. On the other hand, in the quantum mechanics is *not* always possible to distinguish between two arbitrary states. Suppose, for instance, that we what to distinguish the state $|0\rangle$ from state $(|0\rangle + |1\rangle)/\sqrt{2}$. When measured in the computational basis, the first one will give us the value 0 with probability 1. Meanwhile, the second one will return to us 0 with the probability 1/2 and 1 with the equal probability, 1/2. Thus, while a measurement result of 1 implies that the

state must have been $(|0\rangle + |1\rangle)/\sqrt{2}$, since it couldn't have been $|0\rangle$, we can not infer anything about the identity of the quantum state from a measurement result of 0. In the other words, non-orthogonal quantum states cannot be perfectly distinguished [8].

Distinguishing quantum states is an important application of Postulate 3. In order to demonstrate how it is possible to distinguish two different quantum states, we can imagine a metaphor of a game involving two parties, Alice and Bob. Alice chooses a state $|\psi_i\rangle (0 \leq i \leq n)$ from some fixed set of states known to both parties. She gives the state $|\psi_i\rangle$ to Bob, whose task is to identify the index i of the state Alice has given to him.

In this case, we suppose that the states $|i\rangle$ are orthonormal. If Bob defines measurements operators $P_i \equiv |\psi_i\rangle \langle\psi_i|$, one for each possible i, and these operators satisfy the completeness relation, then Bob can prepare the state $|\psi_i\rangle$ to obtain the result i with certainty, since $p(i) = \langle\psi_i| P_i |\psi_i\rangle = 1$. Therefore, he can distinguish the orthonormal states $|\psi_i\rangle$ reliably.

2.2 The density operator

A state vector $|\psi\rangle$ represents a pure state of the quantum system. However, when we want to study an ensemble of quantum states, we introduce an alternate formulation that is mathematically equivalent, the *density matrices*, also called *density operators*, which conceptually take the role of the state vectors discussed so far, as they encode all the (accessible) information about a quantum mechanical system.

2.2.1 Ensembles of quantum states

The density matrix is a practical tool when dealing with mixed states, that describes quantum systems whose state is not completely known. Pure states are those that are characterized by a single state vector (or wavefunction). Mixed states refer to statistical mixtures of pure states, in which we have incomplete information about the system. Suppose we have a quantum system that can be described by a set of states $|\psi_i\rangle$ with respective probabilities p_i. We shall call $\{p_i, |\psi_i\rangle\}$ an *ensemble of pure states*. The density operator for the system is defined by the equation

$$\rho \equiv \sum_i p_i |\psi_i\rangle \langle\psi_i| , \tag{2.18}$$

that is often known as *density matrix*. It turns out that all the postulates of quantum mechanics can be reformulated in terms of the density operator language.

2.2.2 General properties of the density operator

The density matrix is subject to several properties. For instance, ρ is Hermitian (self-adjoint), positive and has trace equal to one. The following theorem illustrates these classes of operators which the density operators are included [9].

Theorem 1 (**Characterization of density operators**). *An operator ρ is the density operator associated to some ensemble $\{p_i, |\psi_i\rangle\}$ if and only if it satisfies the conditions:*

*(1) (**Hermitian adjoint**) $\rho^\dagger = \rho$.*

*(2) (**Trace condition**) ρ has trace equal to one.*

*(3) (**Positivity condition**) ρ is a positive operator.*

Proof. Suppose $\rho \equiv \sum_i p_i |\psi_i\rangle \langle\psi_i|$ is a density operator. Then

$$tr(\rho) = \sum_i p_i tr(|\psi_i\rangle \langle\psi_i|) = \sum_i p_i = 1, \tag{2.19}$$

so the trace condition $\text{tr}(\rho) = 1$ is satisfied. Suppose $|\psi\rangle$ is an arbitrary vector in state space. Then

$$\langle\psi| \rho |\psi\rangle = \sum_i p_i \langle\phi|\psi_i\rangle \langle\psi_i|\phi\rangle = \sum_i p_i |\langle\phi|\psi_i\rangle|^2 \geq 0, \tag{2.20}$$

so the positivity condition is satisfied. □

Suppose ρ is any operator satisfying the trace and positivity conditions. Since ρ is positive, it must have a spectral decomposition

$$\rho = \sum_j \lambda_j |j\rangle \langle j|, \tag{2.21}$$

where the vectors $|j\rangle$ orthogonal, and λ_j are real, non-negative eigenvalues of ρ. The trace condition requires that $\sum_j \lambda_j = 1$. Thus, a system in state $|j\rangle$ with probability λ_j will have

density operator ρ. That is, the ensemble $\lambda_j, |j\rangle$ is an ensemble of states giving rise to the density operator ρ [8].

2.2.3 The postulates of quantum mechanics reformulated

The Theorem 1 allows us to reformulate the postulates of quantum mechanics in the density operator picture as follows [8]:

Postulate 1: Associated to any isolated physical system is a complex vector space with inner product known as the *state space* of the system. The system is completely described by its *density operator*, which is a positive operator ρ with trace one, acting on the state space of the system. If a quantum system is in the state ρ_i with probability p_i, then the density operator for the system is $\sum_i p_i \rho_i$.

Postulate 2: The evolution of a *closed* quantum system is described by a *unitary transformation*. That is, the state ρ of the system at time t_1 is related to the state ρ' of the system at time t_2 by a unitary operator U which depends only on the times t_1 and t_2,

$$\rho' = U \rho U^\dagger. \tag{2.22}$$

Postulate 3: Quantum measurements are described by a collection M_m of *measurement operators*. These are operators acting on the state space of the system being measured. The index m refers to the measurement outcomes that may occur in the experiment. If the state of the quantum system is ρ immediately before the measurement, then the probability that result m occurs is given by

$$p(m) = \text{tr}(M_m^\dagger M_m \rho), \tag{2.23}$$

and the state of the system after the measurement is

$$|\psi'\rangle = \frac{M_m \rho M_m^\dagger}{tr(M_m^\dagger M_m \rho)}. \tag{2.24}$$

The measurement operators satisfy the *completeness relation*,

$$\sum_m = M_m^\dagger M_m = I. \tag{2.25}$$

Chapter 3

Quantum computation

Quantum computation is already a reality [10]. In the last decades, many technological advances in various areas have enabled the development of faster processors [11] that have crossed the threshold that separated the classical from the quantum domain. In classical computation, information is transmitted in *bits* form - that is, it takes the value of 0 or 1 - and is processed through simple logic gates (`AND`, `OR`, `NOT`) that act on one or two bits at a time. At any point in this computation, a classic state is totally determined by the states of all its bits, such that a n-bit computer can exist in one of $2n$ possible states, from 00...00 to 11...1 .

The power of the quantum computer lies in its vast repertoire of states. A quantum computer also has *bits*, but instead of 0 or 1, the *qubits* can represent 0, 1, or any linear combination of both, which is possible through a property known as a **superposition**.

A quantum computer takes advantage of this superposition, which exponentially allows many logical states at once, all states from $|00...0\rangle$ to $|11...1\rangle$, what enables it to perform mathematical calculations that would last many years on a classic computer in just a few seconds. This is an extraordinary feat that no classical computer could achieve. The vast majority of these quantum superpositions, and some of the most useful for quantum computation, are in the form of *entangled* states — that is, they are states that do not correspond to the assignments of digital or analog states of their individual *qubits*.

3.1 Entanglement theory

Composite systems

When we have a system in which there are several quantum objects that interact with each other, we say that this system has *composite states*. For example, a proton that interacts with an electron. When we make a direct product of two systems, we can assume that they were prepared independently of each other. In this case, we say that states are separable and it can be characterized by a *tensor product*

$$|\Phi\rangle = |\phi_A\rangle \otimes |\phi_B\rangle = |\phi_A \phi_B\rangle \,. \tag{3.1}$$

However, for interacting systems, we must consider an internal product in which each element of one state interacts with elements of the other state. Thus, we have a *correlated* (or non-separable) state that cannot be written as a tensor product as in the previous case. We can then write

$$|\Phi\rangle \neq |\phi_A\rangle \otimes |\phi_B\rangle \tag{3.2}$$

Such a state is also known as *entangled state*. Furthermore, the state $|\psi_A\rangle$ lives in the first subspace and state $|\psi_B\rangle$ lives in the second.

3.2 Quantum bits and quantum coherence

3.2.1 What is a Qubit?

In classical computation, we have a system based on *bits*, which get values 0 or 1. The main difference between classical and quantum computation is that in the second one we have this system of *qubits* (quantum bits) that may assume the $|0\rangle$ and $|1\rangle$ states and also a *superposition* of theses two states, in which is not possible to say that the qubit is definitely in the state $|0\rangle$, or definitely in the state $|1\rangle$.

The *qubit* is the simplest quantum mechanical system, the basic unit. It has a two-dimensional state space, where $|0\rangle$ and $|1\rangle$ form an orthonormal basis for that state space. Then an arbitrary

state vector in the state space can be written as a form of linear combinations of states, often called superpositions:

$$|\psi\rangle = a\,|0\rangle + b\,|1\rangle\,, \tag{3.3}$$

where a and b are complex numbers. With the *normalization condition* for state vector, we must have $\langle\psi|\psi\rangle$ = 1 and $|a|^2 + |b|^2$ = 1. The special states $|0\rangle$ and $|1\rangle$ are known as *computational basis states*.

Because of normalization condition seen before, $|a|^2 + |b|^2 = 1$, we can rewrite Eq. 3.3 as

$$|\psi\rangle = e^{i\gamma}(\cos\frac{\theta}{2}\,|0\rangle + e^{i\varphi}\sin\frac{\theta}{2}\,|1\rangle), \tag{3.4}$$

where θ, φ and γ are real numbers. We can ignore the factor of $e^{i\gamma}$ because it has *no observable effects*, and for that reason we can effectively write

$$|\psi\rangle = \cos\frac{\theta}{2}\,|0\rangle + e^{i\varphi}\sin\frac{\theta}{2}\,|1\rangle\,. \tag{3.5}$$

The numbers θ and φ define a point on the unit three-dimensional sphere, as shown in Figure 3.1. This sphere is often called the *Bloch sphere*; it provides a useful means of visualizing the state of a single qubit, and often serves as an excellent testbed for ideas about quantum computation and quantum information [8].

In the classical world, objects exist regardless of whether we observe them or not. Or at least, that's what apparently happens. If I have a coin and throw it up, when it falls on the palm of my hand I observe that I can have two possibilities: either heads or tails up. Therefore, the information I get from this experiment is easy to assimilate. Both states of the coin already existed before I even threw it up. In the quantum world, however, things are not so intuitive, because only after performing a measurement on my system, it takes a certain value. That is, the measurement characterizes the resulting state. Prior to this, the quantum coin existed in some state of heads/tails up or something in between. This superposition of states is odd and counterintuitive, but that's exactly how qubits behave.

Many different physical systems can be used to realize qubits, such as the two different

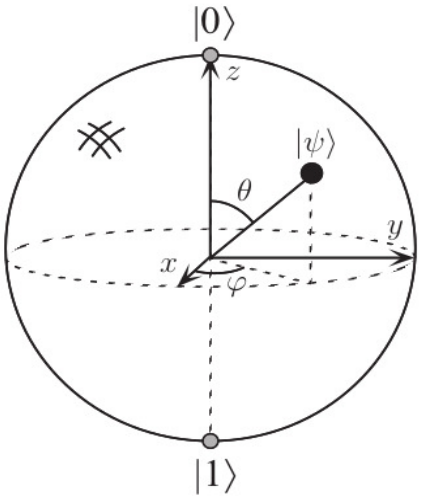

Figure 3.1: Bloch sphere representation of a qubit. *Source: See Ref.[8]*

polarizations of a photon [12]; as the alignment of a nuclear spin in a uniform magnetic field (phenomenon of nuclear magnetic resonance) [13]; as two states of an electron orbiting a single atom [8] such as shown in Figure 3.2. In this model, $|0\rangle$ is the "ground" state, and $|1\rangle$ the "excited" state. By shining polarized light on the atom, for an appropriate length of time and with appropriate energy, it is possible to change the electron state from $|0\rangle$ to $|1\rangle$ and vice versa.

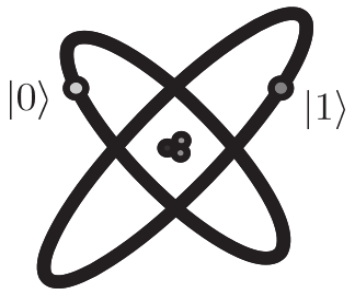

Figure 3.2: Qubit represented by two electronic levels in an atom. *Source: See Ref.[8]*

We can control the time we shine the light, in such way that an electron initially in the state $|0\rangle$ can be moved 'halfway' between $|0\rangle$ and $|1\rangle$, into the state called $|+\rangle$, given by $\frac{1}{\sqrt{2}}|0\rangle + \frac{1}{\sqrt{2}}|1\rangle$.

3.2.2 Multiple qubits

Suppose we have a two qubit system, then would be four possible states, or *computational basis states*, denoted $|00\rangle$, $|01\rangle$, $|10\rangle$ and $|11\rangle$. Because a pair of qubits can also exist in superpositions of these four states, each one of the computational basis states involves a complex coefficient - also called an *amplitude*. Thus, the most general state vector describing these two qubits is

$$|\psi\rangle = \alpha_{00}\,|00\rangle + \alpha_{01}\,|01\rangle + \alpha_{10}\,|10\rangle + \alpha_{11}\,|11\rangle\,. \tag{3.6}$$

If we take a measurement of this state, we get one of these four results: x = 00, 01, 10 or 11, with the state of the qubits after the measurement being $|x\rangle$. The probability is $|\alpha_x|^2$ and under the normalization condition, all the probabilities sum to one. For example, let's say I want to measure the first qubit. The result gives 0 with probability $|\alpha_{00}|^2 + |\alpha_{01}|^2$. The post-measurement state will be

$$|\psi'\rangle = \frac{\alpha_{00}\,|00\rangle + \alpha_{01}\,|01\rangle}{\sqrt{|\alpha_{00}|^2 + |\alpha_{01}|^2}}. \tag{3.7}$$

The Bell state or EPR pair is an important two qubit state, described by

$$\frac{|00\rangle + |11\rangle}{\sqrt{2}}. \tag{3.8}$$

When we measure the first qubit, the result is 0 with probability 1/2. This is exactly the same probability given when the second qubit is measured with result 1. In the first case, the post-measurement state will be $|\psi'\rangle = |00\rangle$, and in the second one, $|\psi'\rangle = |11\rangle$. That is, the measurement outcomes are *correlated*.

In the general case, we may consider a system of n qubits. The computational basis states of this system are of the form $|x_1x_2...x_n\rangle$. A quantum state of such a system is specified by 2^n amplitudes.

3.2.3 Quantum coherence

Generally speaking, *coherence* refers to correlation properties that exist between physical quantities of a wave, or between several waves, or a wave package. When two waves are perfectly coherent, they have a constant phase difference and the same frequency and waveform. This allows *interference* between waves. In the limiting case, interference can be *constructive* or *destructive*.

Some objects we study in quantum mechanics have properties of a wave. Therefore, they are subject to coherence. When an incident electron beam is represented by a pure quantum state, the separation of that beam is represented as a superposition of the pure states representing each of the split beams [14]. A perfectly coherent state has a *density matrix* (also called the "density operator", as we have seen in Chapter 2) that is a projection onto the pure coherent state and is equivalent to a wave function, while a mixed state is described by a classical probability distribution for the pure states that form the mixture.

Quantum coherence has been shown to be equivalent to quantum entanglement [15] in the sense that entanglement measures can be constructed from coherence measures and vice versa.

3.3 Quantum computation

By using the language of *quantum computation*, we can describe changes occurring to a quantum state. Analogous to the way a classical computer is built from an electrical circuit containing wires and logic gates, a quantum computer is built from a *quantum circuit* containing wires and elementary *quantum gates* to carry around and manipulate the quantum information.

3.3.1 Single qubit operations

In the classical case, only one non-trivial single bit gate exists, the `NOT` gate, whose operation is defined by its *truth table*, in which $0 \rightarrow 1$ and $1 \rightarrow 0$, that is, the 0 and 1 states are interchanged. An analogous quantum `NOT` gate for qubits can be defined by the same process, which took the state $|0\rangle$ to the state $|1\rangle$, and vice versa. Specifying the logical operation performed on the qubits $|0\rangle$ and $|1\rangle$ is simple and intuitive, but what about a superposition of these two states? In this case, we need further knowledge about the properties of quantum gates. In

fact, the quantum NOT gate acts *linearly*, that is, it takes the state

$$\alpha |0\rangle + \beta |1\rangle \tag{3.9}$$

to the corresponding state in which the role of $|0\rangle$ and $|1\rangle$ have been interchanged,

$$\alpha |1\rangle + \beta |0\rangle . \tag{3.10}$$

This linear behavior is a general property of quantum mechanics, and very well motivated empirically; moreover, nonlinear behavior can lead to apparent paradoxes such as time travel, faster-than-light communication, and violations of the second laws of thermodynamics.

The linearity of quantum gates allow us to represent them in a matrix form. Thus, suppose we define a matrix X to represent the quantum NOT gate as follows

$$X \equiv \begin{bmatrix} 0 & 1 \\ 1 & 0 \end{bmatrix} . \tag{3.11}$$

If the quantum state $\alpha |0\rangle + \beta |1\rangle$ is written in a vector notation as

$$\begin{bmatrix} \alpha \\ \beta \end{bmatrix} , \tag{3.12}$$

with the top entry corresponding to the amplitude for $|0\rangle$ and the bottom entry the amplitude for $|1\rangle$, then the corresponding output from the quantum NOT gate is

$$X \begin{bmatrix} \alpha \\ \beta \end{bmatrix} = \begin{bmatrix} \beta \\ \alpha \end{bmatrix} . \tag{3.13}$$

As we can see, quantum gates acting on a single qubit can be described by two-by-two matrices. However, there are some constraints on what matrices may be used as quantum gates. It turns out that the appropriate condition on the matrix representing the gate is that the matrix U describing the single qubit gate be *unitary*, that is $U^\dagger U = I$, where $U^\dagger$ is the *adjoint* of U, and I is the two-by-two identity matrix. For example, for the NOT gate it is easy to verify that $X^\dagger X = I$.

In contrast to the classical case, there are many non-trivial single qubit gates. Two important ones which we shall use later are the Z gate

$$Z \equiv \begin{bmatrix} 1 & 0 \\ 0 & -1 \end{bmatrix}, \tag{3.14}$$

which leaves $|0\rangle$ unchanged, and flips the sign of $|1\rangle$ to give $-|1\rangle$, and the *Hadamard* gate,

$$H \equiv \frac{1}{\sqrt{2}} \begin{bmatrix} 1 & 1 \\ 1 & -1 \end{bmatrix}. \tag{3.15}$$

This gate turns a $|0\rangle$ into $(|0\rangle + |1\rangle)/\sqrt{2}$, 'halfway' between $|0\rangle$ and $|1\rangle$, and turns $|1\rangle$ into $(|0\rangle - |1\rangle)/\sqrt{2}$, which is also 'halfway' between $|0\rangle$ and $|1\rangle$. However, H^2 is not a gate, since that $H^2 = I$.

In the Bloch sphere picture, it turns out that single qubit gates correspond to rotations and reflections of the sphere. The Hadamard operation is just a rotation of the sphere about the $\hat{y}$ axis by $\pi/2$, followed by a rotation about the $\hat{x}$ axis by π, as illustrated in Figure 3.3.

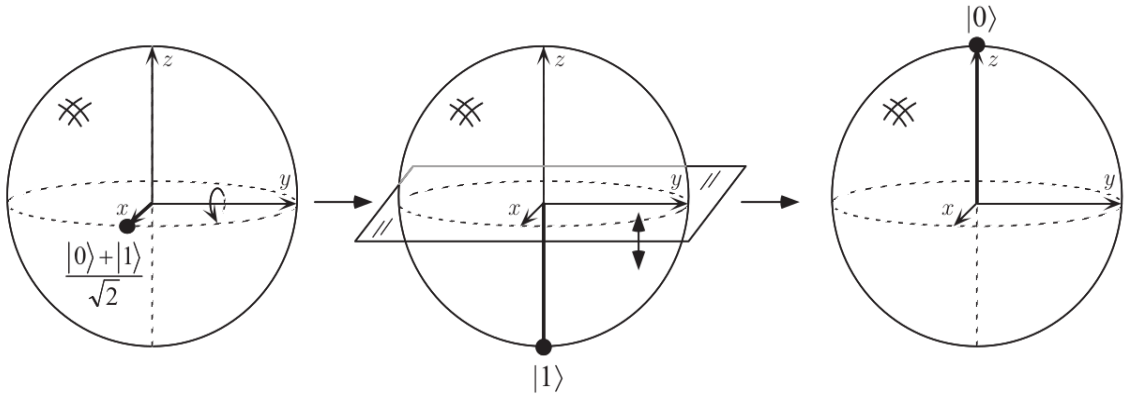

Figure 3.3: Visualization of the Hadamard gate on the Bloch sphere, acting on the input state $(|0\rangle + |1\rangle)/\sqrt{2}$. *Source: See Ref. [8]*

Some important single qubit gates are shown in Figure 3.4, and contrasted with the classical case.

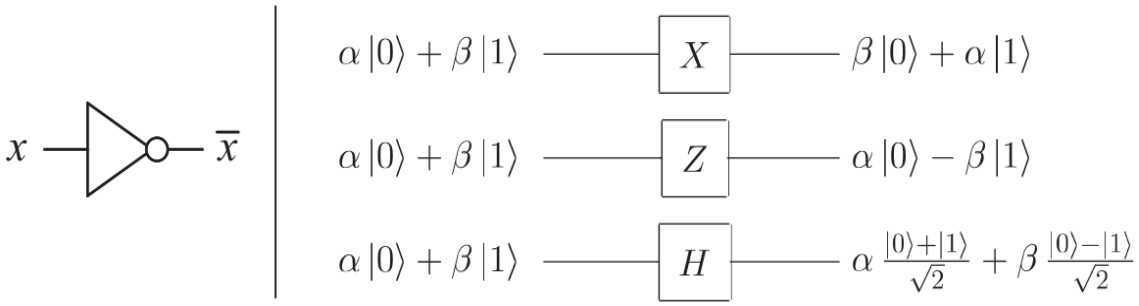

Figure 3.4: Single bit (left) and qubit (right) logic gates. *Source: See Ref.[8]*

3.3.2 Controlled operations and measurement

Controlled-CNOT

In classical logic circuit theory, it is well known that any multi-bit logic operation can be represented by NAND gate compositions, which is known as the universal gate. Figure 3.5 shows the main multi-bit logical gates: OR, AND, NAND, XOR and NOR. The quantum logic gate for operating multiple qubits is the *controlled*-NOT gate, or CNOT. This gate has two input qubits, known as the *control* qubit and the *target* qubit, respectively. The circuit of CNOT is represented in the top right of Figure 3.5; the top line represents the control qubit, while the bottom line represents the target qubit.

If the control qubit is set to 0, then the target qubit is left alone. If the control qubit is set to 1, then the target qubit is flipped. This operation is shown by the following relations.

$$|00\rangle \rightarrow |00\rangle\,; |01\rangle \rightarrow |01\rangle\,; |10\rangle \rightarrow |11\rangle\,; |11\rangle \rightarrow |10\rangle\,. \tag{3.16}$$

The matrix representation is another way of describing the operation that CNOT executes. The first column of U_{CN} describes the transformation that occurs to $|00\rangle$, and similarly for the other computational basis states, $|01\rangle$, $|10\rangle$, and $|11\rangle$. The probability is conserved, because U_{CN} is a unitary matrix, that is, $U_{CN}^{\dagger}U_{CN} = I$.

Even as the NAND gate for the classical logic, the CNOT gate is the *universal* quantum gate. *Any multi-qubit logic gate may be composed from CNOT and single qubit gates* [8].

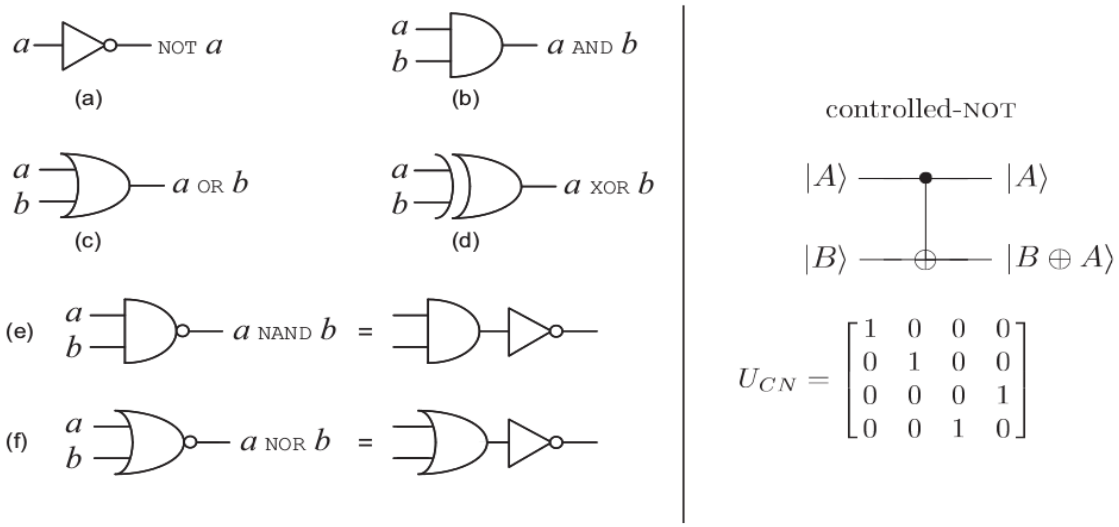

Figure 3.5: On the left are some standard single and multiple bit gates, while on the right is the prototypical multiple qubit gate, the CNOT. The matrix representation of the CNOT, U_{CN}, is written with respect to the amplitudes for $|00\rangle$,$|01\rangle$,$|10\rangle$, and $|11\rangle$, in that order.*Source: See Ref.[8]*

Toffoli gate

One of the most important features of logic circuit theory is the ability to operate bits with different logic gates. Any circuit can be replaced by an equivalent circuit that contains only reversible elements. In the case of quantum circuits, this reversibility operation is performed by the *Toffoli* gate. It is also known as the "controlled-controlled-not" (CCNOT) gate, which describes its action. It has 3-bit inputs and outputs; if the first two bits (*control bits*) are both set to 1, it inverts the third bit (*target bit*), otherwise all bits stay the same. By applying the Toffoli gate twice to a set of bits has the effect $(a, b, c) \to (a, b, c \oplus ab) \to (a, b, c)$, and thus the Toffoli gate is a reversible gate, since it has an inverse – itself.

SWAP

A simple but useful task is swapping the states of the two qubits. The sequence for this operation is described as follows:

$$\begin{aligned} |a, b\rangle \quad &\longrightarrow |a, \oplus b\rangle \\ &\longrightarrow |a \oplus (a \oplus b), a \oplus b\rangle = |b, a \oplus b\rangle \\ &\longrightarrow |b, (a \oplus b) \oplus b\rangle = |b, a\rangle \, . \end{aligned} \tag{3.17}$$

Inputs			Outputs		
a	b	c	a'	b'	c'
0	0	0	0	0	0
0	0	1	0	0	1
0	1	0	0	1	0
0	1	1	0	1	1
1	0	0	1	0	0
1	0	1	1	0	1
1	1	0	1	1	1
1	1	1	1	1	0

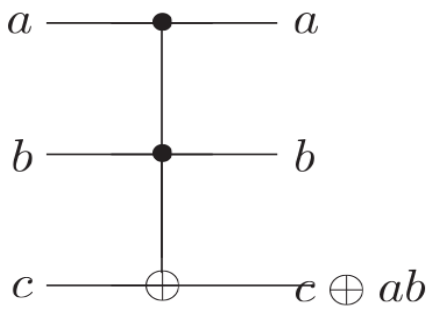

Figure 3.6: Truth table for the Toffoli gate, and its circuit representation. *Source: See Ref.[8]*

The representation of this circuit is in Figure 3.7.

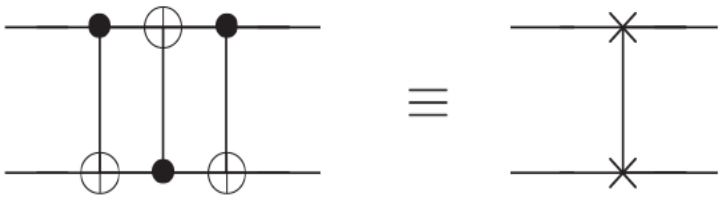

Figure 3.7: Circuit swapping two qubits, and an equivalent schematic symbol notation for this common and useful circuit. *Source: See Ref.[8]*

Measurements

Another important operation is measurement, which we represent by a "meter" symbol, as shown in Figure 3.8. This operation converts a single qubit state $|\psi\rangle = \alpha|0\rangle + \beta|1\rangle$ into a probabilistic classical bit M (distinguished from a qubit by drawing it as a double-line wire), which is 0 with probability $|\alpha|^2$, or 1 with probability $|\beta|^2$.

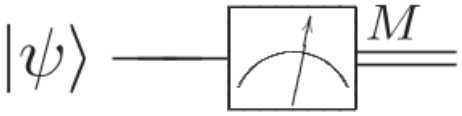

Figure 3.8: Quantum circuit symbol for a measurement. *Source: See Ref.[8]*

Example: Bell states

We may consider four computational basis states as the inputs. By applying a Hadamard gate followed by a `CNOT`, these states are transformed into Bell states, or ERP pairs

$$|\beta_{xy}\rangle \equiv \frac{|0, y\rangle + (-1)^x |1, \overline{y}\rangle}{\sqrt{2}}, \tag{3.18}$$

where $\overline{y}$ is the negation of y.

In	Out
$\|00\rangle$	$(\|00\rangle + \|11\rangle)/\sqrt{2} \equiv \|\beta_{00}\rangle$
$\|01\rangle$	$(\|01\rangle + \|10\rangle)/\sqrt{2} \equiv \|\beta_{01}\rangle$
$\|10\rangle$	$(\|00\rangle - \|11\rangle)/\sqrt{2} \equiv \|\beta_{10}\rangle$
$\|11\rangle$	$(\|01\rangle - \|10\rangle)/\sqrt{2} \equiv \|\beta_{11}\rangle$

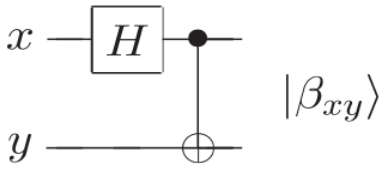

Figure 3.9: Quantum circuit to create Bell states, and its input–ouput quantum truth table. *Source: See Ref.[8]*

Chapter 4

The Nuclear Magnetic Resonance setup

The Nuclear Magnetic Resonance (NMR) technique is based on the use of a static magnetic field together with radio frequency (RF) pulses to control the dynamics of nuclear spins [16]. The NMR spectrometer allows us to characterize and/or prepare the quantum state of the analyzed system, implement logical operations and consequently perform quantum algorithms through unitary transformations. It is also possible through these tools to monitor the evolution of quantum system states, among other potentialities.

4.1 General principles - Nuclear magnetic momentum

We are interested in magnetic systems that have angular momentum. As examples, we have electrons and nuclei of atoms. A system such as a nucleus may consist of many particles coupled together so that in any given state, the nucleus has a total magnetic momentum $\vec{\mu}$ and a total angular momentum $\vec{J}$. In fact the two quantities are proportional

$$\vec{\mu} = \gamma \vec{J}, \tag{4.1}$$

where γ is called "gyromagnetic ratio". In quantum mechanics, the *nuclear total angular momentum* is usually called *nuclear spin*. It is a vector operator that is usually represented by $\hbar\vec{I}$, where $\vec{I}$ is a dimensionless operator representing the total angular momentum of the nucleus, and it is characterized by a quantum number I, called the *nuclear spin quantum number*.

Therefore, the magnetic dipole moment can be directly related to the nuclear spin, according to:

$$\vec{\mu} = \gamma \hbar \vec{I}. \tag{4.2}$$

The quantum characteristics of the spin nuclear operator are given by the eigenvalues and eigenvectors of its square modulus (denoted by $\vec{I}^2$) and its z-component (denoted by I_z) [17]

$$\vec{I}^2 \left| I, m \right\rangle = I(I+1) \left| I, m \right\rangle \tag{4.3}$$

$$I_z \left| I, m \right\rangle = m \left| I, m \right\rangle \tag{4.4}$$

The state vectors denoted by $|I, m\rangle$, correspond to the common eigenvectors of $\vec{I}^2$ and I_z, being specified by the quantum numbers I and m_I, with $m_I = -I, -I+1, ..., I-1, I$. For instance, a proton has a spin quantum number of $I = \frac{1}{2}$, then there are only two possible orientations related to the applied static magnetic field, with $m_I = +\frac{1}{2}, -\frac{1}{2}$. The nuclei of the ^{14}N, ^{19}F and ^{31}P have the spin quantum number I =1, with m_I =1,0,-1. Some nuclei have I =0, for example, ^{12}C and ^{16}O. These atoms are insensible to presence of a magnetic field.

The raising and lowering operators, which are defined from the transverse components of the spin operator respectively by $I_+ = I_x + iI_y$ and $I_- = I_x - iI_y$. The actions of such operators on the $|I, m\rangle$ vectors are given by [17]

$$I_+ \left| I, m \right\rangle = \sqrt{I(I+1) - m(m+1)} \left| I, m+1 \right\rangle \tag{4.5}$$

$$I_- \left| I, m \right\rangle = \sqrt{I(I+1) - m(m-1)} \left| I, m-1 \right\rangle \tag{4.6}$$

4.2 Simple Resonance Theory

Resonance is the name given to a physical phenomenon that occurs when material objects or oscillating fields are at the same natural frequency of vibration [18]. Due to constructive interference and increased vibration amplitude, the total system energy increases. This always happens in Nature, and in the laboratory, we can replicate the necessary conditions for resonance in the most diverse systems. Specifically, when a particle with magnetic dipole momentum is placed in the presence of an external magnetic field and an electric field oscillating at a specific frequency, energy absorption/emission may occur. This phenomenon, named *magnetic resonance*, is present in many closely related techniques such as electron spin resonance, nuclear magnetic resonance, ferromagnetic resonance, and nuclear quadrupole resonance, among others [16].

The application of a static magnetic field $\vec{B}$ on a nuclear spin system produces an interaction between the system and the magnetic field. This interaction is expressed by the Hamiltonian operator

$$\mathcal{H} = -\vec{\mu} \cdot \vec{B}. \tag{4.7}$$

By considering a static magnetic field represented by $B_0\vec{k}$, applied along the z-direction, we can rewrite the Hamiltonian $\mathcal{H}$ as follows:

$$\mathcal{H} = -\gamma\hbar B_0 I_z, \tag{4.8}$$

with I_z being the z-component of the nuclear spin operator $\vec{I}$. Since any component of $\vec{I}$ operator commutes with $\vec{I}^2$ and, consequently, with the nuclear Zeeman Hamiltonian expressed by Eq. (4.7), we may specify simultaneously the eigenstates of I_z, $\vec{I}^2$ and $\mathcal{H}$. These eigenstates are designated by the kets $|I, m_I\rangle$.

The eigenvalues E_m of the Hamiltonian $\mathcal{H}$ are simple, being only multiples of the eigenvalues of I_z. Therefore the allowed energies are

$$E_m = -\gamma\hbar B_0 m_I. \tag{4.9}$$

For nuclei with spin $\frac{1}{2}$, we see that $m_I = \pm\frac{1}{2}$, so there are only two energy levels:

$$E_\pm = \pm\frac{1}{2}\gamma\hbar B_0. \tag{4.10}$$

From Eq. (4.10), we can see that the difference between two adjacents levels is equal to $\gamma\hbar B_0$. In the case of nuclei with spin $I = \frac{3}{2}$, according to Eq. (4.9), we have four energy levels, in which every one of them corresponds to a different magnetic momentum orientation related to magnetic field $\vec{B}$. These energy levels may be observed through an absorption spectra, as shown in Figure 4.1.

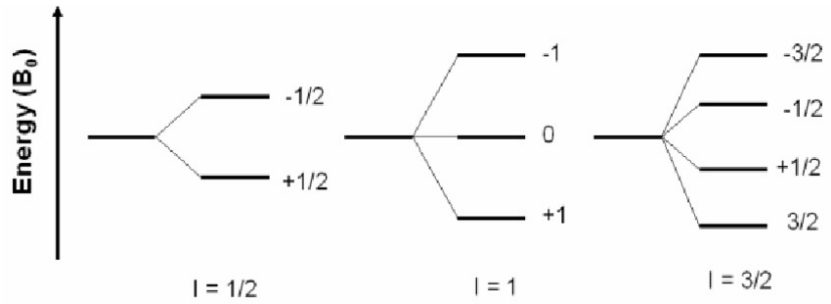

Figure 4.1: Energy level diagram showing the breakdown of nuclear spin degeneracy upon the application of magnetic field. *Source: ResearchGate. [accessed 20 Nov, 2019]*

For energy to be conserved, the interactions that cause these transitions must be time dependent and of such an angular frequency ω that

$$\Delta E = \hbar\omega = \gamma\hbar B_0, \tag{4.11}$$

what allows us to write

$$\omega = \gamma B_0. \tag{4.12}$$

This equation is called *resonance equation*. We may observe that the resonance condition does not depend on the Planck's constant. This fact suggests that the result is closely related to a classical picture. Equation 4.12 may also be written as

$$\omega_L = \frac{\gamma B_0}{2\pi}, \tag{4.13}$$

where ω_L is called **Larmor's frequency**. Classicaly, it is equal to the precession frequency of

the body around the axis of B_0, in complete analogy with the motion of a child's spinning top acted on by the gravitational force (Fig. 4.2). In fact, the higher the static field intensity B_0, the higher the resonance frequency.

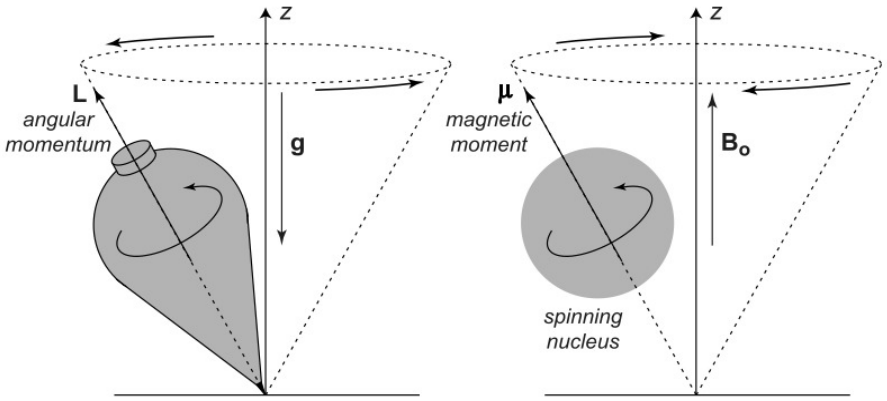

Figure 4.2: Analogy between a spinning top in a gravitational field and a magnetic moment in a magnetic field. *Source: See Ref.[16]*

For an ensemble of identical nuclei in thermal equilibrium, the population of each energy level is given by the Boltzmann distribution [19]. In the case of $I = \frac{1}{2}$, for example, one has a two-level system, with the populations n_- and n_+ of the $m = -\frac{1}{2}$ and $m = +\frac{1}{2}$ levels, respectively, related by the Boltzmann factor:

$$\frac{n_-}{n_+} = e^{-\hbar\omega_L/k_BT}, \tag{4.14}$$

where k_B is the Boltzmann constant and T is the absolute temperature of the ensemble.

Therefore, the effect resulting of the application of a static magnetic field is the appearance of a nuclear magnetization parallel to that field (Fig. 4.3). The thermal equilibrium *magnetization* for an ensemble of nuclei with $I = \frac{1}{2}$, is given by [20, 21]

$$M_0 = \frac{n_0\gamma_n^2\hbar^2 B_0}{4k_BT}, \tag{4.15}$$

where n_0 is the number of nuclei per unit volume. The dependence of the magnetization, increasing linearly with the field strength and inversely proportional to the temperature, is characteristic of the *nuclear paramagnetism*, which is analogous to the electronic paramagnetism, but of magnitude much smaller.

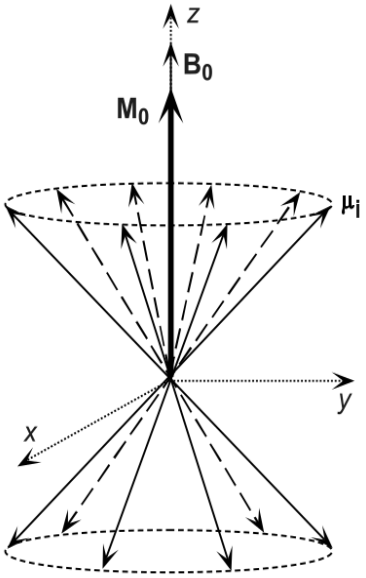

Figure 4.3: Macroscopic magnetization which points to the direction of the field. *Source: See Ref.[16]*

4.3 Radiofrequency field

As we have seen, the term *resonance* implies that we are in tune with a natural frequency of the magnetic system, in this case corresponding to the frequency of gyroscopic precession of the magnetic moment in a external static magnetic field. Because of the analogy between the characteristic frequencies of atomic spectra, and because the magnetic resonance frequencies (Larmor frequencies) fall typically in the radio frequency region (for nuclear spins) or microwave frequency (for electron spins), we often use the terms *radiofrequency* (RF) or *microwave spectroscopy* [21].

When a nuclear spins system already exposed to the action of a static magnetic field $\vec{B}_0$ is placed in the presence of a second magnetic field perpendicular to the first (as in NMR spectrometer), there is a change in the direction of the magnetization of nuclear spins. Thus, the total Hamiltonian of the system is given by the sum of two Hamiltonians,

$$\mathcal{H} = \mathcal{H}_0 + \mathcal{H}_{RF} \tag{4.16}$$

where $\mathcal{H}_{\mathcal{RF}}$ is the Hamiltonian operator associated with the oscillating field $\vec{B}_1(t)$, named *Radiofrequency Hamiltonian*.

For example, if we apply the second field along the x-direction, then $\mathcal{H}_{\mathcal{RF}}$ will be given by

$$\mathcal{H}_{RF} = -\vec{\mu} \cdot \vec{B}_1(t) = -\gamma_n \hbar I_x [2B_1(t) \cos(\Omega t + \phi)], \tag{4.17}$$

where Ω and ϕ are respectively the frequency and the phase of the RF field, and the factor 2 is obtained by considering the linearly polarized magnetic field $\mathbf{B}_1(t)$ as composed of two circularly polarized fields of same frequency and amplitude B_1, but precessing around the z-axis in opposite directions [16]

$$\mathbf{B}_1(t) = \mathbf{B}_1^+(t) + \mathbf{B}_1^-(t), \tag{4.18}$$

where

$$\mathbf{B}_1^+(t) = B_1(t)[\cos(\Omega t + \phi)\mathbf{i} + \sin(\Omega t + \phi)\mathbf{j}], \text{and} \tag{4.19}$$

$$\mathbf{B}_1^-(t) = B_1(t)[\cos(\Omega t + \phi)\mathbf{i} - \sin(\Omega t + \phi)\mathbf{j}]. \tag{4.20}$$

On resonance ($\Omega = \omega_L$), the field $\mathbf{B}_1^-(t)$ rotates around the z-axis with the nuclear Larmor precession, while $\mathbf{B}_1^+(t)$ rotates in the opposite sense. When $\mathbf{\Omega} = -\Omega\mathbf{k}$ (named rotating frame), the field $\mathbf{B}_1^-(t)$ is stationary, as well as the nuclear spins, whereas $\mathbf{B}_1^+(t)$ rotates with twice the Larmor frequency.

If Ω is different from ω_L (off-resonance case), there is a precession of the magnetic moments in the rotating frame around an axis defined by an effective magnetic field given by

$$\mathbf{B}_{eff} = \left(B_0 - \frac{\Omega}{\gamma_n}\right)\mathbf{k} + B_1\mathbf{i}' \tag{4.21}$$

where **i**' is a unit vector along the x'-direction in the rotating frame, being it related to the unit vectors in the laboratory-fixed frame by $\mathbf{i}' = \cos(\Omega t + \phi)\mathbf{i} - \sin(\Omega t + \phi)\mathbf{j}$.

The torque on the collection of nuclear spins causes the net magnetization to deviate from the z-direction (Fig. 4.4). In the on-resonance case, the magnetization **M** precesses, in the rotating frame, around the x'-direction with an angular frequency (named *nutation frequency*) with magnitude given by $\omega_1 = \gamma_n B_1$. After the RF field is turned off, the magnetization points to a direction deviated from the z-axis by a nutation angle given by $\theta_p = \gamma_n B_1 t_p$, where t_p is the time interval during which the RF field was turned on. This transient RF field is named a *RF pulse*, and t_p is therefore the *pulse duration*. If $\theta_p = \pi/2$, the magnetization **M** immediately

after the pulse lies in the plane transversal to $\mathbf{B}_0$; this is called a $\pi/2$ pulse. For a π pulse, on the other hand, the magnetization $\mathbf{M}$ is inverted at the end of the time of application of the pulse [16].

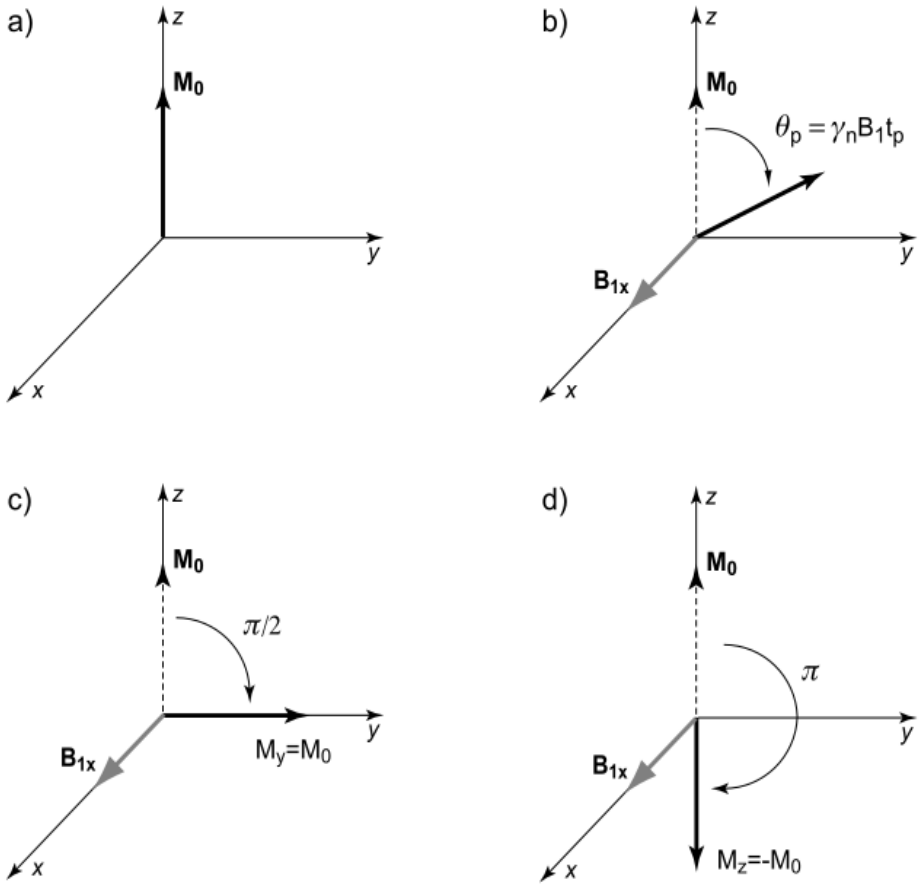

Figure 4.4: The effects of the RF field B_1 on the nuclear magnetization is to drive the magnetization vector away from the z-axis towards the transverse plane. Depending on the amplitude and duration of the RF pulse one can have a $\pi/2$ pulse, a π pulse, or, more generally, a pulse with a nutation angle θ_p. *Source: See Ref.[16]*

In the laboratory frame the magnetization is always precessing around the z-axis, with frequency corresponding to the Larmor frequency. Therefore, after a $\pi/2$ pulse, for instance, there is an alternate electric signal induced by the precessing nuclear magnetization, which can be readily detected by a coil placed in the transversal plane. Basically, this is the signal that is recorded in a conventional pulse NMR experiment. The signal amplitude decays with time after the RF pulse, typically in an exponential way. Thus, the signal is commonly referred to as the

free induction decay (FID), that is, a decaying signal detected in the absence of the excitation RF field.

4.4 Relaxation times

Generally speaking, to describe the behavior of nuclear spins in the presence of a magnetic field, we must be concerned with the interactions of these spins with the neighborhood. "Neighborhood" means the vibrational motion of the crystal lattice in the case of solids, or the Brownian motion of atoms or molecules in the case of liquids. These interactions are responsible for the *relaxation* mechanisms of the spin system.

We have seen that when a set of spins is in thermal equilibrium with its environment, the population of spins at Zeeman energy levels obeys Boltzmann statistics. As a result, lower energy levels are slightly more populated than higher energy levels. Thus, under resonance, energy can be absorbed from the applied radiofrequency field, inducing transitions between them. Associated with the interactions of nuclear spins with their neighborhood, two parameters of great importance should be considered: *longitudinal relaxation time*, T_1, also called *spin-lattice relaxation time*, and *transverse relaxation time* or *spin-spin relaxation time*, T_2. These two parameters are of fundamental importance in the study of magnetic phenomena and can be operationally defined through the Bloch equations [22].

For this, we consider a spins system in thermal equilibrium with its medium, magnetization vector aligned with the statistical magnetic field **B**, applied along the z-direction. Under the thermal equilibrium condition, we have seen that the mean values of M_x and M_y are null and $M_z = M_0$. However, by a process of perturbation of the system Hamiltonian, all three components of the magnetization vector can be considered nonzero at a given time, and the spin relaxation process can be studied.

In 1946, Felix Bloch demonstrated that, in the absence of a radiofrequency field, the components of the magnetization vector are described by the following differential equations [23]

$$d_t M_z = \frac{M_0 - M_z}{T_1}, \tag{4.22}$$

$$d_t M_x = -\frac{M_x}{T_2} \tag{4.23}$$

and

$$d_t M_y = -\frac{M_y}{T_2}. \tag{4.24}$$

After applying a RF pulse such that $\theta_p = \gamma_n B_1 t_p = 90°$, the solution of Eq. (4.22) is expressed by

$$M_z(t) = M_0 \left(1 - e^{-\frac{t}{T_1}}\right). \tag{4.25}$$

From this equation, we see that M_z returns to the thermal equilibrium condition, as illustraded in Fig. (4.5). If at the initial moment we make a magnetization inversion, applying an RF pulse with a duration t_p such that $\theta_p = \gamma_n B_1 t_p = 180°$, the solution of Eq. (4.22) will be

$$M_z(t) = M_0 \left(1 - 2e^{-\frac{t}{T_1}}\right) \tag{4.26}$$

and the thermal equilibrium condition is achieved in a exponential curve shown in the second graph of the Fig. (4.5).

We consider now the transversal relaxation. Again, by taking the spins system in thermal equilibrium after applying a pulse of $\pi/2$ along the x' axis in the rotary axis system, it is possible to demonstrate that the solution of Eq. (4.24) is expressed by

$$M_y(t) = M_0 e^{-\frac{t}{T_2}}. \tag{4.27}$$

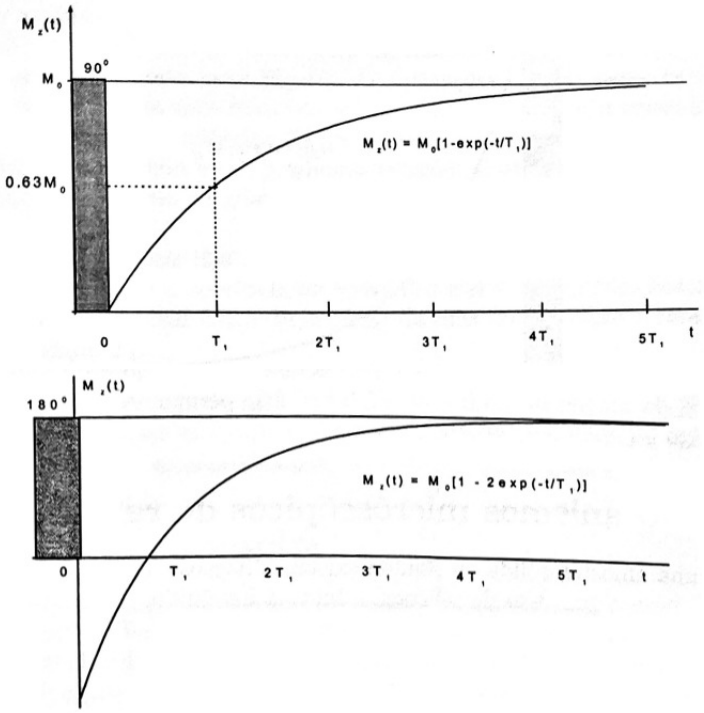

Figure 4.5: Return of magnetization to thermal equilibrium condition after application of a RF pulse of $\pi/2$ and π. *Source: See Ref.[22]*

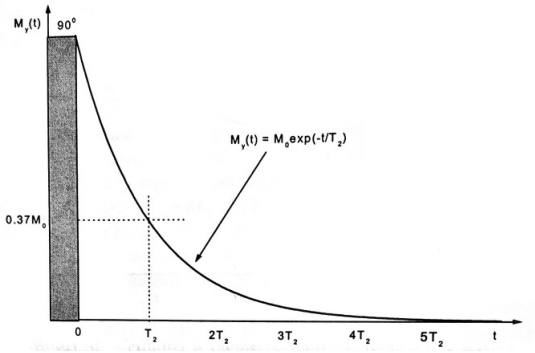

Figure 4.6: Exponential decay of transversal magnetization after application of a RF pulse of $\pi/2$. *Source: See Ref.[22]*

Chapter 5

Applications

In general, the reading operation after the execution of a quantum algorithm is coded in one of the system states in the computational basis, but the execution of an individual quantum logic gate usually involves the creation of many quantum coherencies, which can be considered a crucial rule for the algorithm. In many occasions it is necessary to know all the elements of the density matrix that characterize a quantum system; building this matrix by experimental means is a process called Quantum State Tomography (QST) [24].

The density matrix mapping of a quantum system provides a way to extract the maximum information available, and allows some applications, such as (i) testing the preparation of quantum states, (ii) monitoring the implementation of quantum gates in intermediate steps, (iii) estimating experimental errors and calculating the fidelity of a quantum gate, (iv) calculating the quantum entropy of individual qubits, (v) characterizing decoherence and dissipation effects in quantum systems, (vi) monitoring the Bloch vector trajectories during a quantum logical operation, etc... [25].

This Chapter demonstrates a brief experimental study regarding the basic aspects of quantum information processing via Nuclear Magnetic Resonance (NMR), performed by me and colleagues from other universities at the 4^a EAFExp[1], held at CBPF, Rio de Janeiro, in February 2019.

[1] 4^a Escola Avançada de Física Experimental (CBPF-RJ).

5.1 Quantum State Tomography via Nuclear Magnetic Resonance

The first method of Quantum State Tomography via Nuclear Magnetic Resonance (NMR-QST) was developed by Chuang *et al* [26] and optimized by Long *et al* [27] for systems of heteronuclear molecules (target atoms) with coupled nuclear spins 1/2. This method basically consists of performing a set of specific rotations on the different nuclear spins through the RF pulses and reconstructing the density matrix from the resulting NMR spectra. This method was later adapted for homonuclear coupled spins 1/2 (two or more similar target atoms) [28]. Later, the method was applied for quadrupolar spin 3/2 systems [29], but in this case the non-selective pulses have been replaced by selective RF pulses for the transition.

5.1.1 The experimental setup

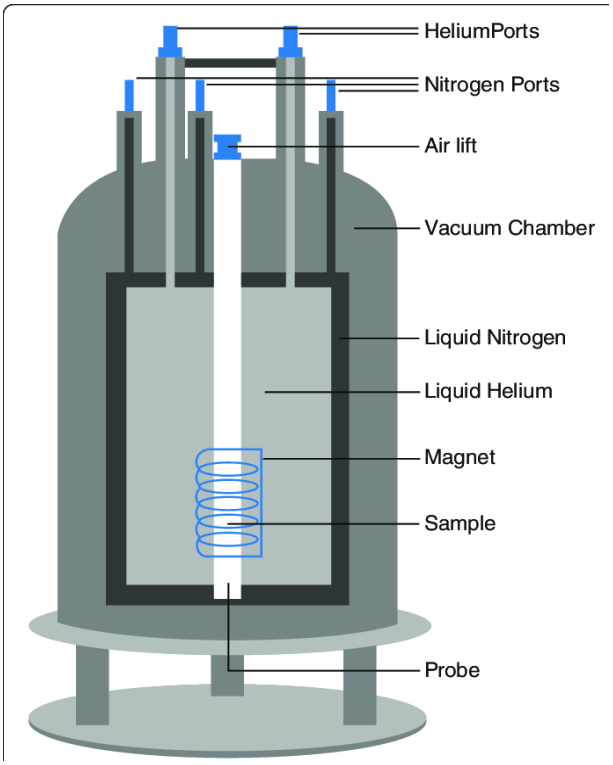

Figure 5.1: Schematic diagram detailing the main components of a nuclear magnetic resonance (NMR) spectrometer. *Source: ResearchGate. [accessed 21 Nov, 2019]*

The spectrometer used in the execution of our work is composed of superconducting coils (magnets) responsible for generating a static magnetic field of up to 20 T (tesla); in our case the intensity was 11.7 T. To produce a magnetic field of this magnitude, an electrical current greater than 100 A is required. One of the advantages of using superconducting wires is that this material can withstand intense electrical currents without causing any resistance, however the disadvantage is that this material must be cooled to temperatures around 4 K. With this, the superconducting wire coil is immersed in a reservoir containing liquid helium, which has a boiling point of 4.18°C. The helium reservoir is thermally insulated by a large reservoir of liquid nitrogen, which has a boiling 77 K. These two reservoirs are separated by vacuum barriers.

To generate the radiofrequency pulses, we determine in a computer the duration, amplitude, resonance frequency and the phase of the pulse. The information is transferred from the computer to an electronic circuit. However, this circuit produces an electrical signal, but the radiofrequency pulses used in NMR are magnetic fields. To produce the magnetic field, we use coils of wires that are placed inside the probe. When passing through these coils, the electrical signal produces an oscillating magnetic field.

With the probe used in the spectrometer, we can apply radiofrequency pulses; detect the signal emitted by a sample at the end of a pulse sequence; control the temperature of the sample; and even rotate the sample (in this case, we used chloroform). The probe is predominantly made of non-magnetic materials, so as not to interfere with the measurements.

5.1.2 Hamiltonian simulation via RMN

The Hamiltonian that determines the natural temporal evolution of the sample in the NMR spectrometer is given by

$$\mathcal{H}_N = \frac{\pi\hbar}{2} J(\sigma_z \otimes \sigma_z), \tag{5.1}$$

where $\hbar$ is Planck's constant and J is the coupling constant between the atoms which form the molecule. The application of radiofrequency pulses in the sample generates a contribution to the natural Hamiltonian as follows

$$\mathcal{H}_{RF} = \hbar\omega_1(n_x\sigma_x + n_y\sigma_y). \tag{5.2}$$

Here, n_x and n_y corresponds respectively to the number of pulses applied in the *x*-direction and the *y*-direction. The state $|\Psi\rangle$ evolves according to the equation

$$|\Psi(t)\rangle = e^{-i\mathcal{H}t/\hbar}\,|\Psi(0)\rangle\,, \tag{5.3}$$

where

$$\mathcal{H} = \mathcal{H}_N + \mathcal{H}_{RF}. \tag{5.4}$$

As seen before, we can define an operator U that performs the temporal evolution of the system, such that

$$U = e^{-i\mathcal{H}t/\hbar}. \tag{5.5}$$

The main idea of the digital approach for quantum computation is the applications of suitable pulses sequences in order to simulate the evolution of a target Hamiltonian from the natural one. We illustrate this in two examples.

The simulation consists of finding U_{RF} such that it satisfies Eq.(5.7) and translating it into a sequence of radiofrequency pulses to be applied to the sample.

Experimental Implementation

Let us first consider the Heisenberg Hamiltonian, which is given by

$$\mathcal{H} = \hbar\omega(\sigma_x \otimes \sigma_x + \sigma_y \otimes \sigma_y + \sigma_z \otimes \sigma_z) \tag{5.6}$$

The central idea is to use the Suzuki-Trotter decomposition [30] in order to write

$$e^{-i\mathcal{H}t/\hbar} = \lim_{n\to\infty}\left(e^{-i\sigma_x\otimes\sigma_x t/n\hbar}e^{-i\sigma_z\otimes\sigma_z t/n\hbar}e^{-i\sigma_y\otimes\sigma_y t/n\hbar}\right)^n. \tag{5.7}$$

We can implement each Trotter step by noting that

$$e^{i\pi\sigma_x/2}e^{-i\omega t\sigma_z}e^{-i\pi\sigma_x/2} = e^{-i\omega t\sigma_y}, \tag{5.8}$$

$$e^{-i\pi\sigma_y/2}e^{-i\omega t\sigma_z}e^{i\pi\sigma_y/2} = e^{-i\omega t\sigma_x}, \tag{5.9}$$

as shown in Fig. 5.2.

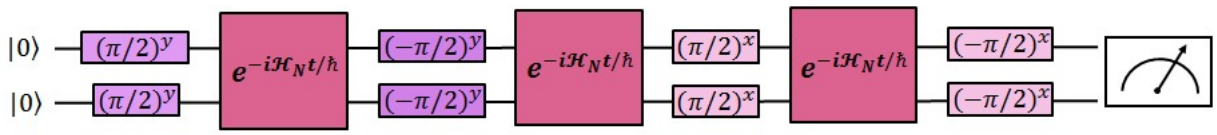

Figure 5.2: Circuit used to simulate Heisenberg's Hamiltonian.

Now, let us consider the Dzyaloshinskii-Moriya Hamiltonian, which is given by

$$\mathcal{H} = \hbar\omega(\sigma_x \otimes \sigma_y + \sigma_y \otimes \sigma_x) \tag{5.10}$$

As before, we use the Suzuki-Trotter decomposition in order to write

$$e^{-i\mathcal{H}t/\hbar} = \lim_{n\to\infty} \left(e^{-i\sigma_x\otimes\sigma_y t/n\hbar} e^{-i\sigma_y\otimes\sigma_x t/n\hbar}\right)^n. \tag{5.11}$$

By using the same relations given in Eqs. (5.8) and (5.9), we get the circuit shown in Fig. 5.3 for each Trotter step.

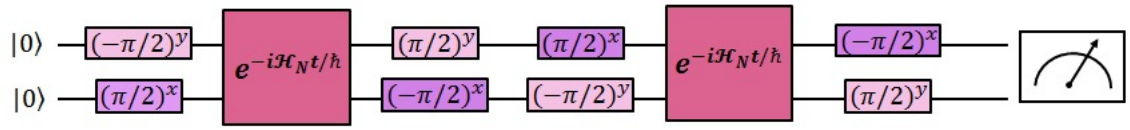

Figure 5.3: Circuit used to simulate the Dzyaloshinskii-Moriya Hamiltonian.

For the experiments, we considered the initial states $|00\rangle$ and $|01\rangle$ for the Heisenberg model while the state $|00\rangle$ was considered in the case of the Dzyaloshinskii-Moriya Hamiltonian. In both cases, we used 2-qubit states.

Results Analysis

For each experiment, 20 measurements were made over 1.48 ms. We use MATLAB ®software features to calculate the system density matrix at each of these time points. Following are the graphs of some of the density matrices obtained for each experiment. These are three-dimensional representations of the density operator, ρ. Each square represents an element of the matrix.

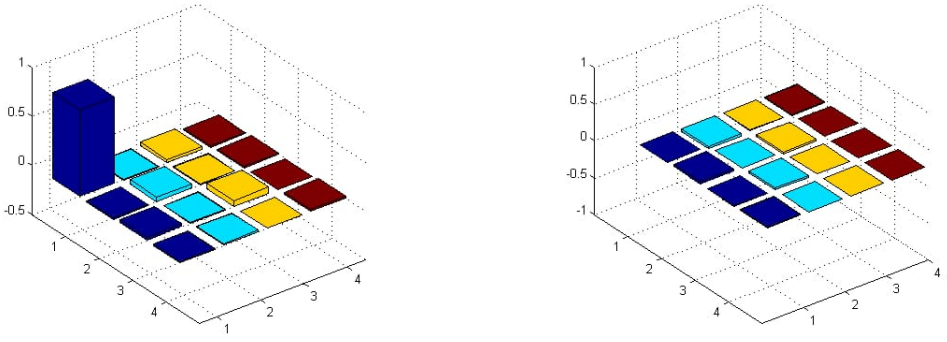

Figure 5.4: Real part (left) and imaginary part (right) of the density matrix for the initial $|00\rangle$ state of Heisenberg's Hamiltonian.

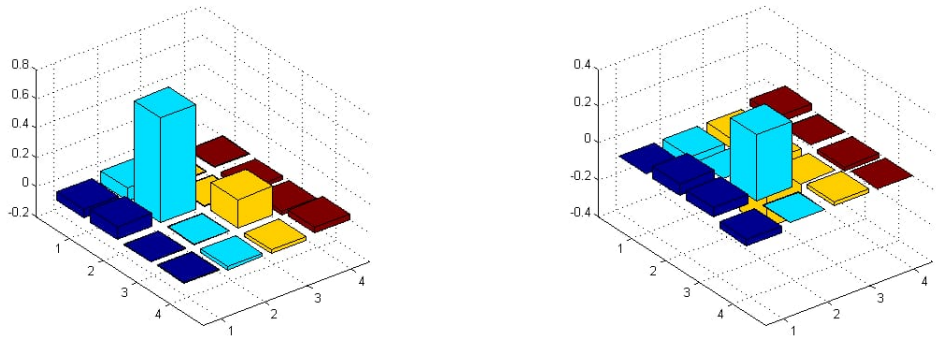

Figure 5.5: Real part (left) and imaginary part (right) of the density matrix for the initial $|01\rangle$ state of Heisenberg's Hamiltonian.

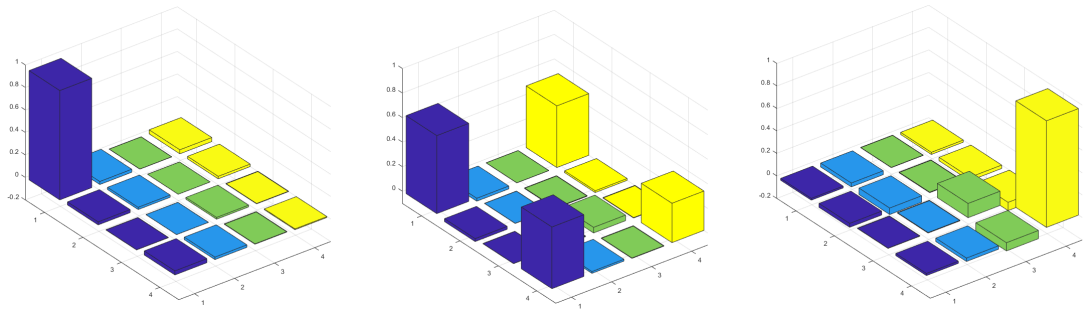

Figure 5.6: Dzyaloshinskii-Moriya simulation: sample states - i) initial ii) after 4 measurements iii) after 9 measurements.

We know that when the density matrix does not change over time, it is because the initial state of the system is an eigenstate of the Hamiltonian; and this is what happens with the state $|00\rangle$ considering the Heisenberg's Hamiltonian, as can be seen in Figure 5.4. However, note that the $|01\rangle$ state density matrix varies over time, not being an Hamiltonian eigenstate, as evidenced in Figure 5.5. Note that the small oscillations that can be observed in the density matrices were considered as experimental errors from NMR magnetic field noise.

On the other hand, the $|00\rangle$ state is not a eigenstate of the Dzyaloshinskii-Moriya Hamiltonian, and therefore, changes in the density matrix over time are observed. The imaginary parts of the density matrices did not show expressive behavior during the temporal evolution under the action of this Hamiltonian, so they were not reproduced here.

An interesting fact to analyze in this experiment is the variation of the entanglement intensity of the system. For this, we use a quantity called *concurrence* [31]. It is a function that quantifies the amount of entanglement present in a quantum state. For a given quantum state with a ρ density matrix, the concurrence is given by

$$C(\rho) = max(0, \lambda_1 - \lambda_2 - \lambda_3 - \lambda_4), \tag{5.12}$$

where λ_i corresponds to the eigenvalues, in descending order, of the Hermitian matrix R given below:

$$R = \sqrt{\sqrt{\rho}\tilde{\rho}\sqrt{\rho}} \tag{5.13}$$

with

$$\tilde{\rho} = (\sigma_y \otimes \sigma_y)\rho^*(\sigma_y \otimes \sigma_y) \tag{5.14}$$

When C =1 entanglement is *maximum*, and when C =0 entanglement is *zero*.

Fidelity, on the other hand, measures the level of similarity between two matrices [32]. For the analysis of the data of this experiment a set of matrices was created with the theoretically predicted values for the temporal evolution of the system under action of the Hamiltonians of Heisenberg and Dzyaloshinskii-Moriya.

If we name the density matrix calculated from the Matlab simulation as ρ_t and the matrix calculated from the experimental data as ρ_e, the fidelity between the quantum states represented by these two matrices will be given by

$$F(\rho_t, \rho_e) = \frac{Tr(\rho_t \rho_e^\dagger)}{\sqrt{Tr(\rho_t \rho_t^\dagger)}\sqrt{Tr(\rho_e \rho_e^\dagger)}}. \tag{5.15}$$

By calculating the fidelity between the measured matrices ρ and the ρ_t matrices, we can measure the accuracy of the results obtained. The maximum fidelity value is 1, which corresponds to the case where the matrices are equal, and its minimum value is 0.

For the concurrence measurement of Heisenberg's Hamiltonian simulation, we had the following results

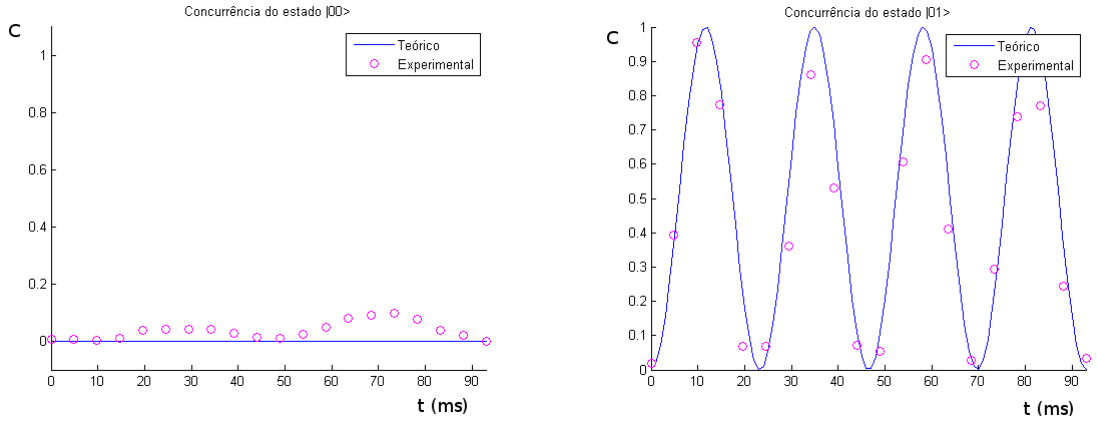

Figure 5.7: Graphs of concurrence for the states $|00\rangle$ and $|01\rangle$.

Figure 5.7 shows that for Heisenberg's Hamiltonian, the concurrence is almost constant over time, for the case where the system state is $|00\rangle$, because this state is a system eigenstate, evidencing that there is no entanglement. However, for the state $|01\rangle$, it is observed that this system is oscillating between 0 and 1, showing that there is a constant entanglement and separation

cycle in the system.

For the Dzyaloshinskii-Moriya Hamiltonian we observe the following behavior

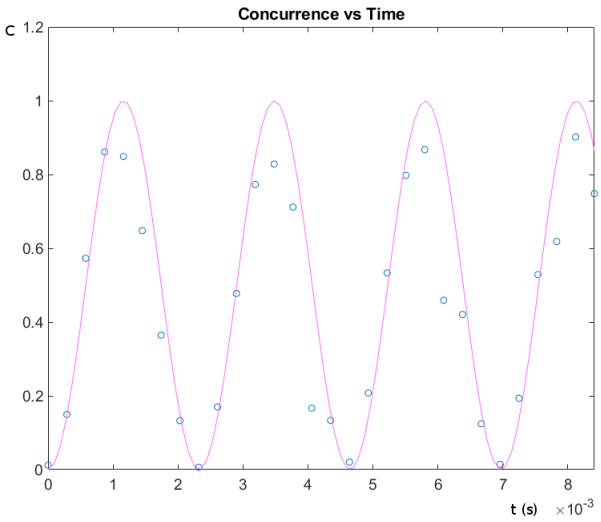

Figure 5.8: Concurrence for the state $|00\rangle$.

We see that for this Hamiltonian, the concurrence ranges from 0 to 1, suggesting that, under its action, the system varies between separable and completely entangled states.

The results of fidelity calculations for Heisenberg's Hamiltonian are given below.

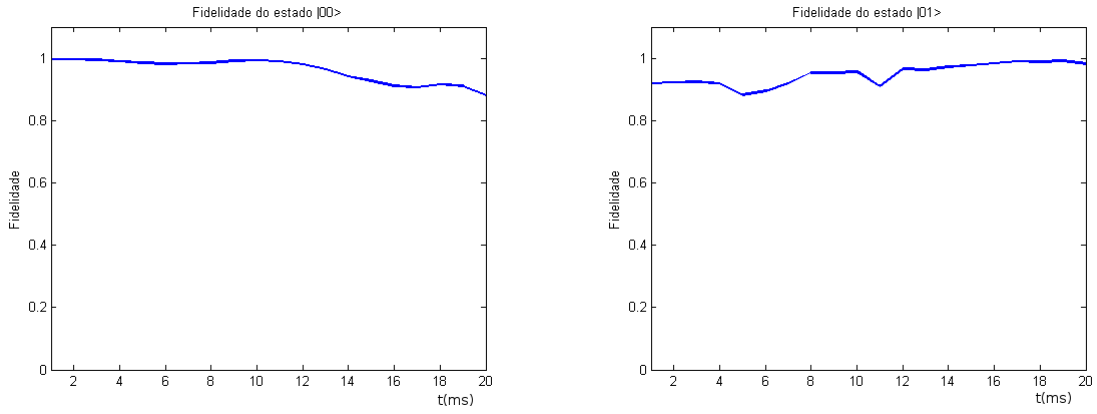

Figure 5.9: Fidelity for the states $|00\rangle$ and $|01\rangle$.

For the Hamiltonian of Dzyaloshinskii-Moriya we obtained:

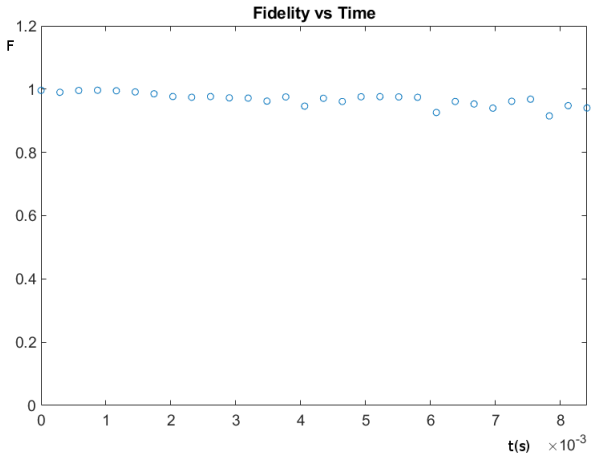

Figure 5.10: Fidelity for the state $|00\rangle$.

For both Hamiltonians we obtained a relatively constant fidelity measure close to 1, which suggests a good agreement between theory and experiment.

Chapter 6

Conclusions

Using numerical, experimental and analytical tools, we were able to develop circuits and radiofrequency pulse sequences that would properly simulate the proposed Hamiltonian. The results had a good agreement between theory and experiment, which can be seen by comparing the theoretically predicted densities matrices and the data, both by observation and by calculating the quantum state fidelity. In addition, we were able to understand the operations of the NMR spectrometer, the elaboration of quantum circuits and other more general concepts of quantum mechanics. Throughout this work, we realized the Nuclear Magnetic Resonance (NMR) as a powerful and versatile tool for creating and manipulating quantum states. The processes we implemented demonstrated the great potential of the NMR technique in quantum information processing and consequently some of the possibilities of connection between NMR and Quantum Computation.

As we can see in the second part of Chapter 5, this example of applying a quantum algorithm in practice provides us with a very significant experience regarding the study of the tools offered by Quantum Computation to solve the most varied mathematical problems. Numerous other examples could be cited, such as factoring algorithms and other statistical analysis that can be used in various areas of science. Quantum Computing is a booming area that still has many challenges, especially in its physical structure and engineering, however, it is increasingly essential for the continuous construction of human knowledge.

All of this work was a set of brief, but quite enriching, experiments on the field of computer science and quantum information, but not just that. For me, it was the gathering of elements from various disciplines of study in my Physical Engineering course, such as Quantum Physics,

Logic Circuits, Experimental Techniques, Statistics, etc., and everything that makes a good physical scientist, added from travel to other cities in the country and a network of new friends and future co-workers. These trips, provided through the joint efforts of researchers from the host institutions, were essential for choosing the theme of this monograph and my future area of expertise in the master's degree.

Bibliography

[1] R. P. Feynman, "Simulating physics with computers," *International journal of theoretical physics*, vol. 21, no. 6, pp. 467–488, 1982.

[2] J. Preskill, "Quantum computing and the entanglement frontier," *arXiv preprint arXiv:1203.5813*, 2012.

[3] A. W. Harrow and A. Montanaro, "Quantum computational supremacy," *Nature*, vol. 549, no. 7671, p. 203, 2017.

[4] C. S. Calude and E. Calude, "The road to quantum computational supremacy," *arXiv preprint arXiv:1712.01356*, 2017.

[5] P. M. M. Duhem, *The aim and structure of physical theory*, vol. 13. Princeton University Press, 1991.

[6] M. Jammer *et al.*, *The conceptual development of quantum mechanics*. McGraw-Hill New York, 1966.

[7] A. Peres, *Quantum theory: concepts and methods*, vol. 57. Springer Science & Business Media, 2006.

[8] M. Nielsen and I. L. Chuang, *Quantum Computation and Quantum Information*. Cambridge: Cambridge University Press, 2000.

[9] K. Husimi, "Some formal properties of the density matrix," *Proceedings of the Physico-Mathematical Society of Japan. 3rd Series*, vol. 22, no. 4, pp. 264–314, 1940.

[10] C. Monroe and J. Kim, "Scaling the ion trap quantum processor," *Science*, vol. 339, no. 6124, pp. 1164–1169, 2013.

[11] F. Arute, K. Arya, R. Babbush, D. Bacon, J. C. Bardin, R. Barends, R. Biswas, S. Boixo, F. G. Brandao, D. A. Buell, *et al.*, "Quantum supremacy using a programmable superconducting processor," *Nature*, vol. 574, no. 7779, pp. 505–510, 2019.

[12] T. Wilk, S. C. Webster, H. P. Specht, G. Rempe, and A. Kuhn, "Polarization-controlled single photons," *Phys. Rev. Lett.*, vol. 98, p. 063601, Feb 2007.

[13] R. R. Ernst, G. Bodenhausen, A. Wokaun, *et al.*, *Principles of nuclear magnetic resonance in one and two dimensions*, vol. 14. Clarendon press Oxford, 1987.

[14] R. Feynman and R. Leighton, "B. and sands, m.,(1963), the feynman lectures on physics vol. 3."

[15] K. C. Tan and H. Jeong, "Entanglement as the symmetric portion of correlated coherence," *Phys. Rev. Lett.*, vol. 121, p. 220401, Nov 2018.

[16] I. Oliveira, R. Sarthour Jr, T. Bonagamba, E. Azevedo, and J. C. Freitas, *NMR quantum information processing*. Elsevier, 2011.

[17] C. Cohen-Tannoudji, B. Diu, and F. Laloë, *Quantum mechanics*. Wiley, 1977.

[18] E. D. Glendening and F. Weinhold, "Natural resonance theory: I. general formalism," *Journal of computational chemistry*, vol. 19, no. 6, pp. 593–609, 1998.

[19] F. Reif, *Fundamentals of statistical and thermal physics*. Waveland Press, 2009.

[20] M. E. Smith, "Ap guimaraes. magnetism and magnetic resonance in solids. john wiley & sons, chichester, 1998, pp. 298, price£ 45.50. isbn 0-471-1977-42," *Magnetic Resonance in Chemistry*, vol. 39, no. 1, pp. 53–54, 2001.

[21] C. P. Slichter, *Principles of magnetic resonance*, vol. 1. Springer Science & Business Media, 2013.

[22] W. Wolney Filho, *Mecânica quântica*. Editora da UFG, 2002.

[23] F. Bloch, "Nuclear induction," *Phys. Rev.*, vol. 70, pp. 460–474, Oct 1946.

[24] U. Leonhardt, H. Paul, and G. d'Ariano, "Tomographic reconstruction of the density matrix via pattern functions," *Physical Review A*, vol. 52, no. 6, p. 4899, 1995.

[25] J. Teles, E. R. deAzevedo, R. Auccaise, R. S. Sarthour, I. S. Oliveira, and T. J. Bonagamba, "Quantum state tomography for quadrupolar nuclei using global rotations of the spin system," *The Journal of chemical physics*, vol. 126, no. 15, p. 154506, 2007.

[26] I. L. Chuang, N. Gershenfeld, M. G. Kubinec, and D. W. Leung, "Bulk quantum computation with nuclear magnetic resonance: theory and experiment," *Proceedings of the Royal Society of London. Series A: Mathematical, Physical and Engineering Sciences*, vol. 454, no. 1969, pp. 447–467, 1998.

[27] G. Long, H. Yan, and Y. Sun, "Analysis of density matrix reconstruction in nmr quantum computing," *Journal of Optics B: Quantum and Semiclassical Optics*, vol. 3, no. 6, p. 376, 2001.

[28] I. L. Chuang, N. Gershenfeld, and M. Kubinec, "Experimental implementation of fast quantum searching," *Physical review letters*, vol. 80, no. 15, p. 3408, 1998.

[29] F. A. Bonk, E. R. deAzevedo, R. S. Sarthour, J. D. Bulnes, J. Freitas, A. P. Guimaraes, I. S. Oliveira, and T. J. Bonagamba, "Quantum logical operations for spin 3/2 quadrupolar nuclei monitored by quantum state tomography," *Journal of Magnetic Resonance*, vol. 175, no. 2, pp. 226–234, 2005.

[30] M. Suzuki, "Improved trotter-like formula," *Physics Letters A*, vol. 180, no. 3, pp. 232–234, 1993.

[31] S. Hill and W. K. Wootters, "Entanglement of a pair of quantum bits," *Physical Review Letters*, vol. 78, p. 5022–5025, Jun 1997.

[32] R. Jozsa, "Fidelity for mixed quantum states," *Journal of modern optics*, vol. 41, no. 12, pp. 2315–2323, 1994.

[33] A. Souza, I. Oliveira, and R. Sarthour, "A scattering quantum circuit for measuring bell's time inequality: a nuclear magnetic resonance demonstration using maximally mixed states," *New Journal of Physics*, vol. 13, no. 5, p. 053023, 2011.

[34] A. Messiah, "Quantum mechanics, volume ii," *Appedix C (Section IV)(North-Holland Publishing Company, Amsterdam, 1969)*, 1962.

[35] E. Farhi, J. Goldstone, S. Gutmann, J. Lapan, A. Lundgren, and D. Preda, "A quantum adiabatic evolution algorithm applied to random instances of an np-complete problem," *Science*, vol. 292, no. 5516, pp. 472–475, 2001.

[36] A. M. Childs, E. Farhi, J. Goldstone, and S. Gutmann, "Finding cliques by quantum adiabatic evolution," *arXiv preprint quant-ph/0012104*, 2000.

[37] A. Einstein, B. Podolsky, and N. Rosen, "Can quantum-mechanical description of physical reality be considered complete?," *Phys. Rev.*, vol. 47, pp. 777–780, May 1935.

[38] N. Bohr, "Can quantum-mechanical description of physical reality be considered complete?," *Physical review*, vol. 48, no. 8, p. 696, 1935.

[39] J. S. Bell, "On the einstein podolsky rosen paradox," *Physics Physique Fizika*, vol. 1, no. 3, p. 195, 1964.

[40] J. F. Clauser, M. A. Horne, A. Shimony, and R. A. Holt, "Proposed experiment to test local hidden-variable theories," *Physical review letters*, vol. 23, no. 15, p. 880, 1969.

Appendices

Appendix A

Other Applications

1.1 Determination of the global phase of a qubit

The global phase described by $e^{i\phi}$ is sometimes ignored experimentally as it does not change the expected value of observables relative to the $|\Psi\rangle$ state. Thus, finding it was considered an experimental challenge. In the execution of the experiment, the theoretical analysis was first performed to find the relation between an arbitrary angle θ and the global phase ϕ. This analysis allowed us to elaborate a quantum circuit, similar to a scattering circuit, soon after this algorithm was 'translated' in terms of RF pulses and implemented in the spectrometer. Such steps are described below.

To find a relation between the global phase and the system, the scattering circuit described in Figure 1.1 was used as a base.

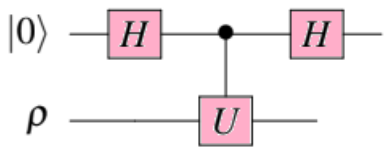

Figure 1.1: Scattering circuit for a qubit $|0\rangle$.

This circuit is very important for quantum computing, with important applications such as testing Bell's time inequality violations [33]. Such a circuit has an interesting feature, the relation $\langle\sigma_z|\sigma_z\rangle = tr(\rho U)$.

Using the circuit of Figure 1.1 for any given qubit $|\Psi\rangle$, after measuring its state after operator U, the tensor τ becomes:

$$|\tau\rangle = \frac{1}{2}(|0\rangle\,|\Psi\rangle + |1\rangle\,U\,|\Psi\rangle). \tag{1.1}$$

In this study, the qubit $|\Psi\rangle$ selected was the $|0\rangle$, then the operator U is $R_z(\theta)$, which is the rotation around z axis. Therefore, $\sigma_x\,|\tau\rangle = \frac{1}{\sqrt{2}}(|0\rangle\,|0\rangle + |1\rangle\,R_z(\theta)\,|0\rangle)$. Thereby, $\langle\tau|\,\sigma_x\,|\tau\rangle$ becomes:

$$\langle\tau|\,\sigma_x\,|\tau\rangle\,\frac{1}{2}((\langle 0|\,\langle 0| + \langle 0|\,R_z(\theta)^\dagger\,\langle 1|)(|1\rangle\,|0\rangle + |0\rangle\,R_z(\theta)^\dagger\,|0\rangle)) \tag{1.2}$$

$$\langle\tau|\,\sigma_x\,|\tau\rangle = \frac{1}{2}(\langle 0|\,\langle 0|0\rangle\,R_z(\theta)\,|0\rangle + \langle 0|\,R_z(\theta)^\dagger\,\langle 1|1\rangle\,|0\rangle) \tag{1.3}$$

$$\langle\tau|\,\sigma_x\,|\tau\rangle = \frac{1}{2}(\langle 0|\,R_z(\theta)\,|0\rangle + \langle 0|\,R_z(\theta)^\dagger\,|0\rangle)\,\langle\sigma_x|\sigma_x\rangle \tag{1.4}$$

$$\langle\sigma_x|\sigma_x\rangle = \frac{1}{2}(\langle 0|\,R_z(\theta)^\dagger + R_z(\theta)\,|0\rangle) \tag{1.5}$$

Similarly, for σ_y, $\sigma_y\,|\tau\rangle = \frac{1}{\sqrt{2}}(-R_z(\theta)i\,|0\rangle\,|0\rangle + i\,|1\rangle\,|0\rangle)$. Thus

$$\langle\tau|\,\sigma_y\,|\tau\rangle = \frac{1}{\sqrt{2}}\,\langle\tau|\,(-R_z(\theta)i\,|0\rangle\,|0\rangle + i\,|1\rangle\,|0\rangle) \tag{1.6}$$

$$\langle\tau|\,\sigma_y\,|\tau\rangle = \frac{(\langle 00| + R_z(\theta)^\dagger\,\langle 0|)}{\sqrt{2}}\,\frac{(-R_z(\theta)i\,|00\rangle + i\,|10\rangle)}{\sqrt{2}} \tag{1.7}$$

By simplifying the Eq.(1.7), we get:

$$\langle\sigma_y|\sigma_y\rangle = \frac{i}{2}(\langle 0|\,R_z(\theta)^\dagger - R_z(\theta)\,|0\rangle) \tag{1.8}$$

Getting the ratio between (1.8) and (1.5), we have that

$$\tan(\phi/2) = \langle\sigma_y|\sigma_y\rangle\,/\,\langle\sigma_x|\sigma_x\rangle \tag{1.9}$$

$$\phi = 2\arctan\left(\frac{\langle\sigma_y|\sigma_y\rangle}{\langle\sigma_x|\sigma_x\rangle}\right) \tag{1.10}$$

Thus, a direct relation between the global phase ϕ and the angle θ of the rotation in z (R_z) can be noted.

Experimental Implementation

In order to find the global phase of a qubit, an interferometry simulation is made so that the global phase can be found. This is done because measurement of the global phase of a system is only possible if a circuit similar to the scattering circuit is used.

In this way, by applying a logic gate to one qubit and making it interact with the other, one can make the global phase similar to a relative phase for a certain 2-level system. Thus, in order to be able to perform such manipulation, the scattering circuit described in the figure below was used.

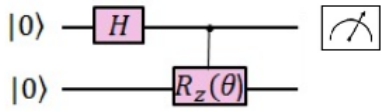

Figure 1.2: Representation of the circuit that was used to observe the global phase of a qubit.

This circuit has among its components a Hadamard quantum logic gate acting on only one qubit ($|0\rangle$) which causes a system entanglement, so that the same starting qubit can be found in both $|0\rangle$ state and $|1\rangle$ state. This operation is represented by the matrix of Hadamard (1.11).

$$H = \frac{1}{\sqrt{2}} \begin{bmatrix} 1 & 1 \\ 1 & -1 \end{bmatrix} \tag{1.11}$$

It is worth noting that this matrix acts on the $|0\rangle$ and $|1\rangle$ states, which can be represented as:

$$|0\rangle = \begin{bmatrix} 1 \\ 0 \end{bmatrix} \tag{1.12}$$

$$|1\rangle = \begin{bmatrix} 0 \\ 1 \end{bmatrix} \tag{1.13}$$

And the second operation done is a controlled logic gate, which acts on the second qubit with the control on the first, giving the second a relative phase of type $e^{i\phi}$.

Results Analysis

Once the translation to radiofrequency pulses of the circuit observed in figure 1.2 was done, 50 data were collected for the system rotation angle θ, ranging from 0 to 4π. Thus, for each data from the sample set analyzed in this challenge, when the tomography technique was finalized, the values of $\langle\sigma_x|\sigma_x\rangle$ and $\langle\sigma_y|\sigma_y\rangle$ were obtained. results are equivalent to magnetizations in x and y, respectively.

With these known values, we can use the equation deduced in item 1 for the relation between the system phase angle and the magnetization of $\langle\sigma_x|\sigma_x\rangle$ and $\langle\sigma_y|\sigma_y\rangle$, observed in (1.10). Thus, a graph is plotted with the results found (Figure 1.3).

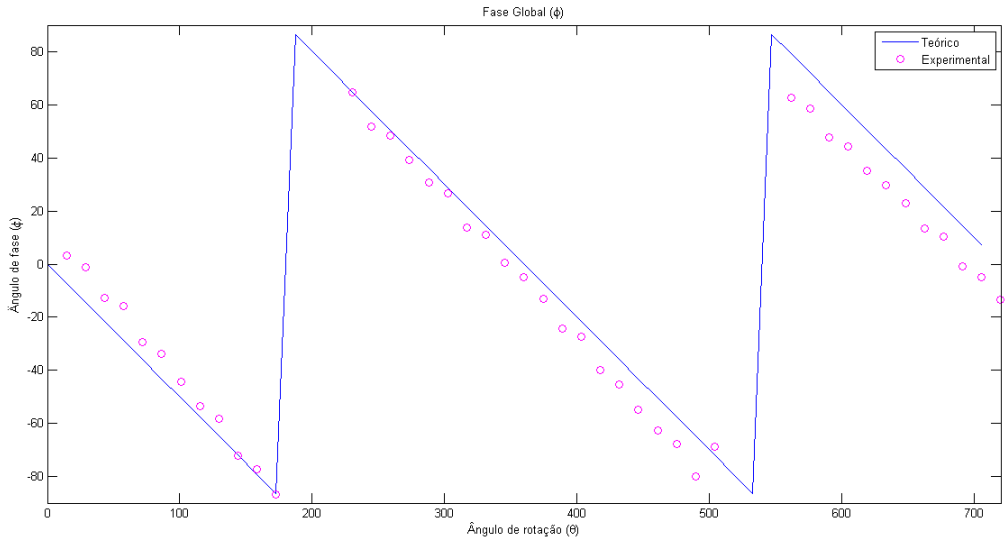

Figure 1.3: Graph of the relationship between phase angle and rotation angle.

Thus, it is concluded that the Eq.(1.10) is effective for observing the global phase of a qubit by relating it to the system rotation.

1.2 Quantum Annealing

The adiabatic quantum mechanical theorem says that when a system evolves according to a Hamiltonian with sufficiently small time variations, that system remains in its instantaneous ground state [34]. This behavior is used in solving certain computational problems, the main example being optimization problems [35, 36]. The challenge to be solved is encoded in a final Hamiltonian H_F, whose ground state is often not easy to find. Adiabatic algorithms begin with the ground state of an initial Hamiltonian H_B which is easy to build and whose ground state is also easy to prepare. The fundamental state of H_B (initial state), which is an overlap of all H_F eigeinstates, evolves according to a Hamiltonian $H(s)$. $H(s)$ is a linear overlap of the initial Hamiltonian H_B and the final Hamiltonian H_F, such that:

$$H(s) = [1 - s(t)]H_B + s(t)H_F \tag{1.14}$$

where $0 \leq s(t) \leq 1$.

Initially the Hamiltonian H_B has all the predominance in the evolution of the state ($s(t) = 0$), as time goes by the Hamiltonian H_F is gaining relevance ($s(t)) > 0$), until H_B is null and H_F dominates evolution ($s(t) = 1$).

Experimental Implementation

Our objective in this part of the work was to obtain and simulate a Hamiltonian performing the classic 3-bit sum using 2 qubits, using the adiabatic quantum computation method. Our first step was to determine a Hamiltonian H_F acting in our initial state, according to equation 1.14 and according to input values (0 or 1) for a, b and c would do the sum of these inputs, eventually provide the appropriate result. Our initial and final Hamiltonians were:

$$H_B = \hbar\omega(\sigma_x \otimes \mathbb{I} + \mathbb{I} \otimes \sigma_x) \tag{1.15}$$

$$H_{\mathrm{F}} = (\sigma_z \otimes \mathbb{I}) sgn\left[\cos(\mathrm{a+b+c})\frac{\pi}{3}\right] + (\mathbb{I} \otimes \sigma_z) sgn\left[\cos(\mathrm{a+b+c})\pi\right] + (\sigma_z \otimes \sigma_z) sgn\left[\cos(\mathrm{a+b+c})\frac{\pi}{2}\right] \tag{1.16}$$

In numerical calculations, we implemented the $s(t)$ parameter according to the

$$s(\text{t}) = \frac{1}{2}\left[\frac{1}{n'}\tan\left(\frac{2n't}{N} - \arctan(\text{n'})\right) + 1\right] \tag{1.17}$$

where $n' = \sqrt{N-1}$.

In the experiments, we performed the increments according to the $T/50$ ratio, where T is the total duration of the experiment. The initial state used was:

$$\left(\frac{|0\rangle + |1\rangle}{\sqrt{2}}\right) \otimes \left(\frac{|0\rangle + |1\rangle}{\sqrt{2}}\right) \tag{1.18}$$

Given the fact that our evolution must take place adiabatically, there are two possibilities for building our circuits and therefore our pulse sequences. We can make each evolution have increases in pulse intensity or free system evolution time. We opted for the method that modifies the pulse intensity with each actuation. Figure 1.4 shows a simplification of what our quantum circuit would be for the case where the sum of the inputs is zero.

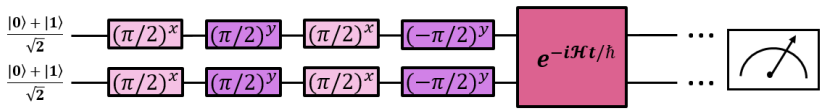

Figure 1.4: Simplified representation of the circuit used in the Hamiltonian simulation of equation 1.14 through the adiabatic quantum method. This pulse sequence was repeated 50 times and each cycle we increased the pulse intensity according to $T/50$. Only at the end of the repetitions did we perform the measurement, so the presence of ellipses in the image.

Results Analysis

As stated earlier, the evolution of our initial state was defined according to the Hamiltonian H_S, which in turn was defined by the binary values of the a, b and c inputs. Figure 1.5 shows the real part of the ρ_0 density matrix corresponding to our final state $|00\rangle$, this state corresponds to the sum of the inputs equal to 0. The left side of the figure represents the ρ_0 prepared experimentally and the right side ρ_3 prepared theoretically. The imaginary parts did not show expressive behavior in our results, so they were discarded.

Figure 1.6 has the same configuration as the previous one, but the results now correspond to the ρ_3 matrix of the $|11\rangle$ state, which is equivalent to the sum of the inputs equal to 3.

The graphs show a good approximation between numerical and experimental results, this shows that our circuits and pulse sequences simulated our Hamiltonian relatively well. An

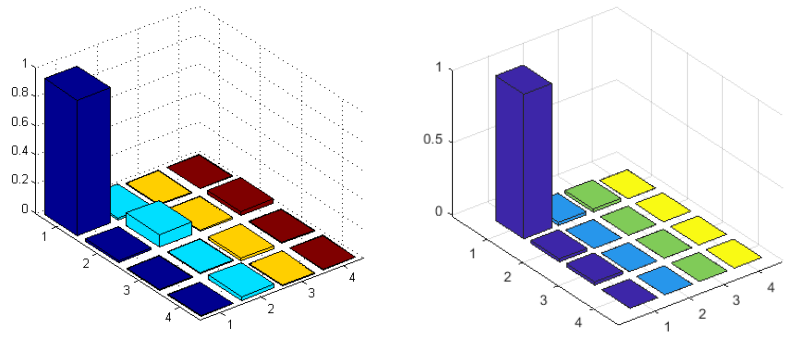

Figure 1.5: Real part of the ρ_0 density matrix corresponding to the state $|00\rangle$, as a result of the sum of the inputs equal to 0: Experimental (left) and theoretical (right)

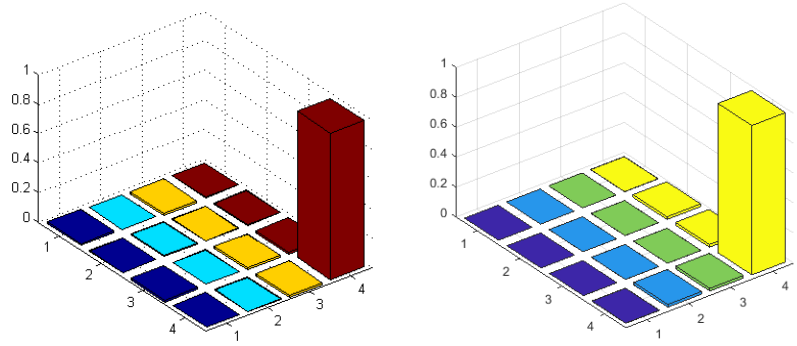

Figure 1.6: Real part of the density matrix ρ_3 corresponding to the state $|11\rangle$, as a result of the sum of inputs of 3: Experimental (left) and theoretical (right)

important observation to make is that these results do not prove or demonstrate that our simulation was adequate or the most efficient; this would require another type of measurement called Process Tomography (full density matrix mapping throughout the evolution of the state). But within the problem proposal, these results correspond to the desired level.

Appendix B

Implementation at the IBM quantum computing system

As part of the final assignment for the *Introduction to Computing and Quantum Information* course grade, an implementation at the IBM quantum computer was undertaken in order to study the Bell's inequalities.

2.1 EPR and Bell's theorem

In 1935, Albert Einstein, Boris Podolsky and Nathan Rosen (EPR) wrote an article entitled "Can Quantum Mechanical Description of Physical Reality Be Considered Complete?", in which they set criteria for identifying whether a physical theory was complete or not, according to the reality of its elements. A sufficient condition for the reality of a physical quantity is the ability of predicting it with certainty without disturbing the system. However, in the case where we have two physical quantities described by non-commuting operators, the knowledge of one precludes the knowledge of the other. According to EPR, this leads to two conclusions: either (1) the wave function does not fully describe the reality of the system, or (2) these two quantities do not have a simultaneous reality [37].

It is important to note that EPR rejected the idea that the measurement of a particle in a entangled pair could affect the state of another particle distant from the first one. They concluded that the particle in question must be described by a complete quantum formalism, thus there will

be a reasonable description (a "local reality") of the world. In order to achieve this, they argued that quantum mechanics should be supplemented by additional variables. These additional, or *hidden*, variables were to restore to the theory causality and locality.

2.1.1 Bohr's principle of complementarity and Einstein locality

On the other hand, Niels Bohr disagreed with EPR's interpretation of the notion of locality. He conceded that *"there is no question of a mechanical disturbance of the system under investigation"* (due to the measurement of the other, distant system), but he added: *"there is essentially the question of an influence on the very conditions which define the possible types of predictions regarding the future behavior of the system"* [38]. Bohr gave to his point of view the name *"complementarity principle"*. Its meaning is that some types of predictions are possible while others are not, because they are related to mutually incompatible tests. According to Bohr, each experimental setup must be considered separately.

Even with these arguments, Einstein was not convinced. For him, what actually happens with one system spatially separated from another, is something independent of what is done with the second one. This physical principle has received the name *Einstein locality*.

2.1.2 Bell's inequalities

In 1964, John Bell showed in an article [39] that if measurements are chosen correctly for a given entangled state, statistics cannot be explained by any theory of local hidden variables, and that there must be correlations that go beyond the classical domain.

For better understanding of the idea of entanglement, suppose that there are two systems (blue and red) and in each of them two measurements are made: A, A', B and B', which generate an output 1 or -1, as shown in Figure 2.1.

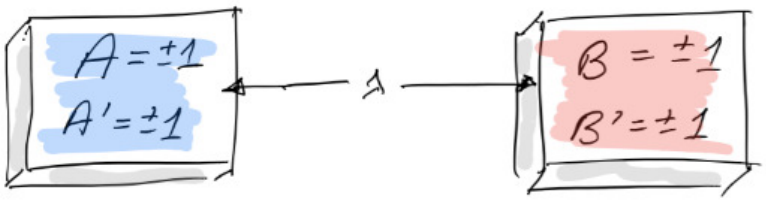

Figure 2.1: Measurement results on the systems blue and red. *Source: IBM©*

Suppose now that a statistical correlations between $A(a)$ and $B(b)$ is due to information carried by and localized within each particle, and that at some time in the past the particles constituting one pair were in contact and communication regarding this information. The information, which is not quantum mechanical, is part of the content of a set of hidden variables, denoted collectively by λ. The results of the two selections are then to be deterministic functions $A(a, \lambda)$ and $B(b, \lambda)$. Since the two selections may occur at an arbitrarily great distance from each other, the **locality** assumption requires $A(a, \lambda)$ to be independent of the parameter b and $B(b, \lambda)$ to be likewise independent of a. No information can travel faster than the speed of light. The hidden variable λ that defines all correlations is such that

$$\langle AB \rangle = \sum_{\lambda} P(\lambda) A(\lambda) B(\lambda). \tag{2.1}$$

Let us define the operator

$$C = \sum_{\lambda} P(\lambda)[A(\lambda)(B(\lambda) - B'(\lambda)) + A'(\lambda)(B(\lambda) - B'(\lambda))]. \tag{2.2}$$

The **realism** assumption requires that all observables have a definite value regardless of the measurement (+1 or -1). This implies that either $|B(\lambda) + B'(\lambda)| = 0$ (or 0) while $|B(\lambda) + B'(\lambda)| \neq 0$ (or 2), respectively. That is, $|C| = 2$, and noise will only decrease this value.

In 1969, John Clauser, Michael Horne, Abner Shimony and Richard Holt derived the CHSH Inequality [40], $|C| \leqslant 2$, such as

$$C = \langle AB \rangle - \langle AB' \rangle + \langle A'B \rangle + \langle A'B' \rangle \tag{2.3}$$

and the correlated expectation is given by

$$\langle AB \rangle = P(1,1) + P(0,0) - P(0,1) - P(1,0) \tag{2.4}$$

with 0 generating an output +1 and 1 generating an output -1. The correlation of 1 means that both observables have even parity, and the correlation of -1 means that both have odd parity.

However, in fact $|C| > 2$. How is this possible? The previous assumptions must not be valid, and this is one of the most counterintuitive ideas to be accepted in the quantum world. In the last section, we will assemble the quantum circuit corresponding to this problem, for better

understanding of what happens and how each observable is measured and combined to give the value of $|C|$.

IBM's quantum computer provides us with a online platform on which we can implement quantum circuits and test the processing power of this tool. *Quantum Composer* is a graphical interface for programming a quantum processor that closely resembles the tools used in composing musical scores, which is nonetheless very interesting. Each line of the circuit represents a quantum state that evolves over time. Numerous specific gates and measurers can be applied to them, representing the mathematical operations and measurements on the system. A very detailed tutorial on how *Quantum Composer* works is given on the IBM' site.[1]

2.1.3 Bell's experiment

The Bell's experiment proposed here uses the entangled state described in Eq.2.5, and the two measurements for system A are Z and X, while the two for B are $W = \frac{1}{\sqrt{2}}(Z + X)$ and $V = \frac{1}{\sqrt{2}}(Z - X)$.

$$\left|\phi^{\pm}\right\rangle = \frac{|00\rangle \pm |11\rangle}{\sqrt{2}} \tag{2.5}$$

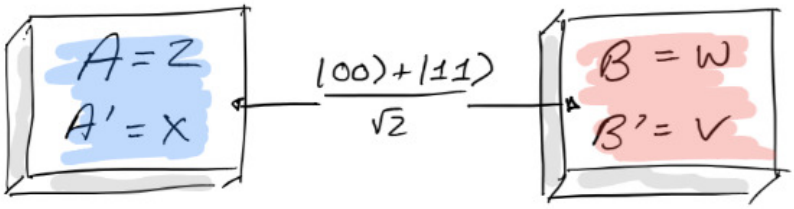

Figure 2.2: Measurement results on systems. *Source: IBM©*

For an optimal implementation, the four correlated expected values would give $\langle ZW\rangle = \langle ZV\rangle = \langle XW\rangle = \frac{1}{2}$ and $\langle XV\rangle = \frac{-1}{2}$, which gives a value of $|C| = 2\sqrt{2}$.

To run this experiment on the quantum processor, we need the following quantum circuit and 4 measurements (Figure 2.3).

In the first part of the experiment, *qubits* are initially prepared in the ground state $|00\rangle$. H leads the first *qubit* to superposition $\frac{|00\rangle+|10\rangle}{\sqrt{2}}$, and the CNOT gate flips the second *qubit* if the

[1]Wadler, D.: IBM Gives Public Cloud Access to New 5-Qubit Quantum Computer, 2016. Accessed June 21,2018.

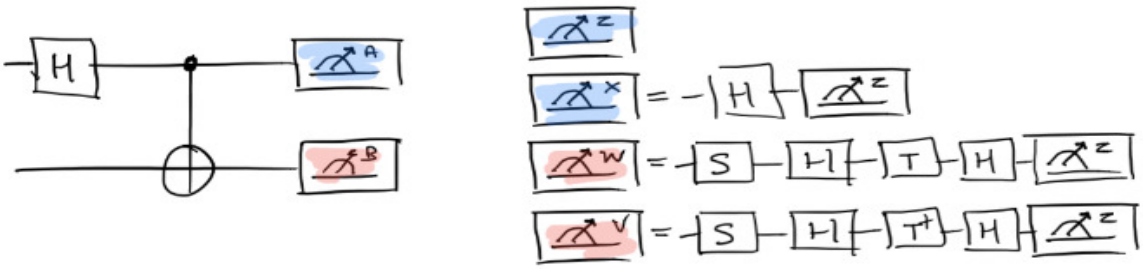

Figure 2.3: Quantum circuit of the Bell's experiment. *Source: IBM©*

first one is excited, going to the state $\frac{|00\rangle+|11\rangle}{\sqrt{2}}$. This is the entangled state (commonly called "Bell state") required for the test. In the first experiment, the measurements are from observables Z and $W = \frac{1}{\sqrt{2}}(Z + X)$. To rotate the base of measurement for the W axis, the sequence of gates S - H - T - H is used, and then it takes place a standard measurement. The correlated $\langle ZW \rangle$ must be close of $\frac{1}{\sqrt{2}}$, and it is found by the equation already described.

In the second experiment, the two observables are Z and $V = \frac{1}{\sqrt{2}}(-X + Z)$. To rotate the base, we use the sequence of gates S - H - $T^\dagger$ - H, and then the measurement is taken. The correlated $\langle ZV \rangle$ is found similarly as before and it should be close to $\frac{1}{\sqrt{2}}$.

Finally, in the third and fourth experiments, $\langle XW \rangle$ and $\langle XV \rangle$ should be close to $\frac{1}{\sqrt{2}}$ and $\frac{-1}{\sqrt{2}}$, respectively. Measurements of W and V are performed as in the previous cases, and X via Hadamard gate before of the standard measurement.

2.1.4 Results Analysis

Using the *Quantum Composer*, all the quantum circuits described previously were implemented (Figure 2.4) and the Table 2.1 shows all probability values in each measurement that was obtained.

Table 2.1: Bell test: 8192 shots - Performed on 6/21/2018 at 6:59 PM.

	P(1,1)	P(1,0)	P(0,0)	P(0,1)	$\langle AB \rangle$
ZZ	0.506	-	0.494	-	-
ZW	0.428	0.076	0.423	0.073	0.702
ZV	0.431	0.076	0.424	0.069	0.710
XW	0.432	0.075	0.423	0.070	0.710
XV	0.072	0.430	0.076	0.422	-0.704

The values of $\langle AB \rangle$ were calculated by Eq. 2.6. Through Eq. 2.7, we have a value of $|C| = 2.826$, which is very close to $|C| = 2\sqrt{2} = 2.828$, with an error of approximately 0.07%. This is a great result that clearly demonstrates how accurate and powerful the quantum computer processing is in practice.

$$\langle AB \rangle = P(1,1) + P(0,0) - P(0,1) - P(1,0) \tag{2.6}$$

$$C = \langle AB \rangle - \langle AB' \rangle + \langle A'B \rangle + \langle A'B' \rangle \tag{2.7}$$

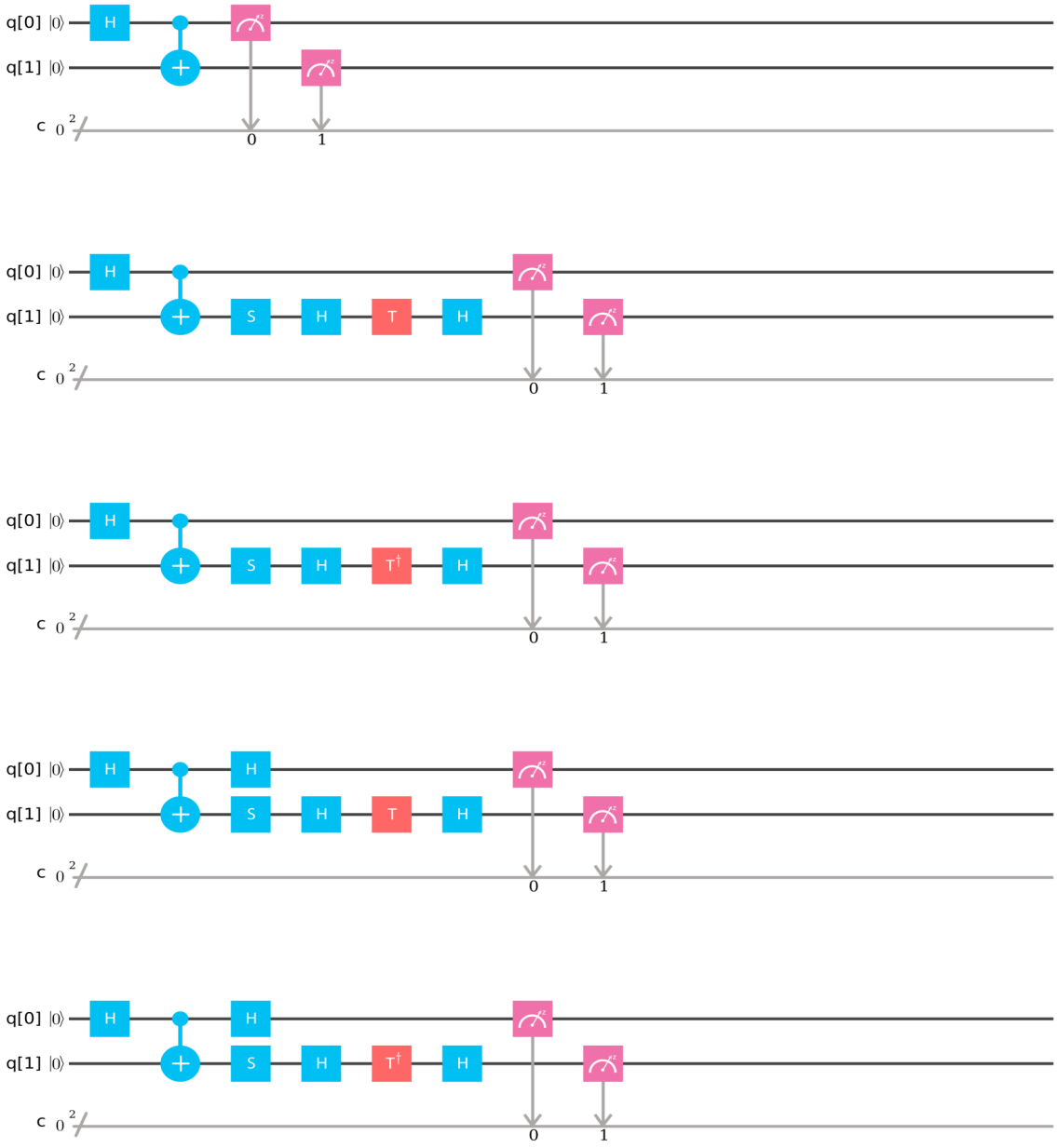

Figure 2.4: Quantum Circuits for Bell States - Measurements for ZZ, ZW, ZV, XW and XV.